LIST OF SYMBOLS

C_0: Initial concentration of gas (kgmole/m^3)

E_i: Activation energy for gas i (J/mol)

h: Heating rate (K/s)

k_i: Rate constant for gas i (s^{-1}·concentration^{1-n})

k_{i0}: Pre-exponential factor for gas i (s^{-1}·concentration^{1-n})

$ki_{0,app}$: Apparent pre-exponential factor for gas i (s^{-1})

M: Molecular weight (kg mole/kg)

n: Reaction order

PPMA: ppm per unit area

R: Universal gas constant (8.314 J/mol·K)

R^2: Correlation coefficient

t: Time (s)

T: Absolute temperature of sample (K)

X_i: Conversion of gas i

Y: Gas concentration in ppm

LIST OF FIGURES

LIST OF TABLES

Chapter 1

Introduction

1.1 Background

Aluminium is produced by electrolysis, and the anodes used for this process are made of carbon. Low carbon (anode) consumption is very important for the aluminum industry which directly affects the cost of production as well as the environmental emissions. The anode consumption is strongly influenced by the properties of anode. In aluminum electrolysis, the study of carbon anode manufacturing and the improvement of its production techniques lead to savings in energy and reduction in gaseous emissions for the aluminum company[1-2].

The role of this international collaboration project is to pioneer the establishment of a research partnership between UQAC, GNU (Guizhou Normal University), and CHALCO (China Aluminum Corporation) in the aluminum technical development field. In addition, this project also aims to create a successful collaboration model called "2+1 partnership": one Canadian university + one Chinese university + one enterprise. In this model, all of the three parties use their expertise to turn the research, development, and manufacturing trinity into a successful reality. This partnership model has already been approved by the Guizhou province government.

1.2 Statement of the Problem

In China, the low carbon consumption economy is a policy to improve the sustainable development. With new economy stimulus plan, states' governments seek to accelerate economic restructuring and desire to make substantial progress in transforming the economy from the extensive system to the technology-focused system. Therefore, all the aluminum companies give importance to energy saving, the reduction of carbon dioxide and other harmful gases during the production process as well as cost reduction, which are clearly linked to the improvement of anode quality. However, Chinese carbon plants have to deal with the raw material deterioration and multiple sources of petroleum coke acquisition at the same time. In addition to the transition from extensive production to technology-focused production, some problems such as equipment aging, high energy consumption, and high operation costs always accompany the technology upgrade of Chinese carbon plants.

The challenge for carbon plants is to produce a consistently high quality product regardless of changes in the actual circumstances and to cope with such variability [3-4]. During the industrial carbon anode manufacturing processes, raw materials play an important role in determining the final product (anode) properties, and the aluminum industry has to deal with the declining quality of the available petroleum coke around the world. Thus, today more and more industries, internally or through collaborative research projects with universities, seek ways to at least maintain the quality of anodes at the current level even under variable raw material conditions.

During the industrial carbon anode manufacturing process, baking step plays an important role in determining the final product (anode) properties. Higher baking temperatures require higher energy consumption. In Chalco Guizhou branch, anodes are baked in the open-type horizontal baking furnace. Such furnaces are very large and necessitate significant fuel consumption. Anodes are placed in pits, stacked in layers from bottom to top, and are surrounded by packing coke. The hot gas in the horizontal flues, heated by heavy oil as well as the combustion of volatiles released during baking, provide the energy for baking. The consumption of fuel is in the order of more than three million Canadian dollars each year. As the world crude oil prices increase, the cost of production keeps rising[5].

In recent years, companies found ways to lower fuel consumption. Better use of the heat content of the binder pitch volatiles is one of the best options for Chalco plant. Theoretically, based on the energy requirement for anode baking, the heat the pitch volatile combustion could provide is more than the amount of heat needed to bake the anodes. Within the flue gas temperature range 200°C to 800°C, anode temperature is increased to around 500°C. Between the temperatures 300°C and 600°C, pitch volatiles, mainly the condensable gas (tar) and non-condensable gases (H_2 and CH_4) are released from the anodes. Then, the volatiles are drawn, under the negative pressure, into the flue in order to provide the energy for anode baking where the temperature of flue is high enough to burn them almost completely. This way, a certain amount of energy could be saved; in the mean time, the quality of products could be maintained by the high temperature level [6-8].

1.3 Scope

For optimizing the anode properties (air permeability, air reactivity, and CO_2 reactivity), first, it was necessary to know the industrial anode production process and its operating system. This would facilitate the assesment of the steps which need improvement and to focus the work along with the results of this assessment. The results of the sampling and testing of the raw materials (coke and pitch), dry aggregate and recycled butt indicated which parts of the process needed attention. The anode quality optimization was based on a large number of single-factor experiments in order to adjust the specific production processes at the laboratory scale. The different production formulations, conditions, and parameters were tested repeatedly. Depending on the results of the series of anode formulation experiments, the anode recipe which yield the best anode quality was used in the second part. The correlation between the baking conditions and anode properties were studied in order to find the baking conditions which will improve anode properties further. Also, experimental results helped identify the anode baking conditions that would lead to energy saving during baking via the volatile release characterisation. Finally, the technical results and findings were implemented in the plant operation after the necessary technology transfer.

Anode quality is affected by the anode recipe and the anode baking conditions. The studies are very important on the both categories. In this study, a scanning electron microscopy and energy dispersive X-ray spectroscopy (SEM-EDS) were used in order to optimize the anode recipe. Then, the most costly anode manufacture process – anode

baking were discussed after the anode formulation part in this dissertation. The CO_2 and air reactivities and air permeability were measured to evaluate carbon anodes in this research because not only they relate to anode density but also to anode consumption. This helped assess the potential for saving energy and reducing CO_2 and hazardous gas emissions of the carbon production process.

Upon correlation with the results of anode formulation tests, the sample which has the best properties was chosen to simulate the baking process in the laboratory, and the gas produced (tar, H_2 and CH_4) was analyzed. Their amounts were also calculated not only to be able to find the conditions to improve the quality, but also to determine the possibility of using the condensable (tar) and non-condensable gases (H_2 and CH_4) to reduce the energy consumption and to improve the furnace efficiency.

1.4 Objectives

The global objective of the project is to improve the quality of the presently used carbon anodes. The raw materials used during anode preparation were analyzed by taking the local conditions into account in order to optimize the anode formulation. The relation between anode recipes and the anode properties such as CO_2 reactivity, air reactivity, and air permeability were studied. The specific objectives are:

1. Test the properties of anode such as CO_2 reactivity, air reactivity, and air permeability for different paste formulations and anode baking conditions.
2. Correlate the effect of anode preparation conditions and anode baking conditions

with anode reactivity.

3. Analyse the kinetics of devolatilisation of condensable and noncondensable gas for each anode baking condition.

4. Transfer the findings to the plant for industrial application.

Chapter 2

Literature review

2.1 Anode Manufacture Process

During pre-baked anode manufacturing process, normally there are four basic steps:

Raw material handling;

Dry aggregate preparation;

Preheating, mixing, and paste cooling;

Forming and anode cooling.

The calcined coke and recycled butts are crushed, screened, and sized to prepare the required size distribution and are mixed to form a dry aggregate. This aggregate is then preheated to between 110°C and 165°C and mixed with around 15 wt% pitch at a temperature between 150°C and 230°C. This process is called the 'anode paste preparation' and the result is the 'anode paste', which is then formed into an anode block either by pressing or vibratory compaction. Then, the 'green anode' is cooled and stored for baking[10]. After baking, the pre-baked anode is ready to be used in the electrolysis cell. A process flow sheet of Chalco plant is shown in Figure 2.1[11].

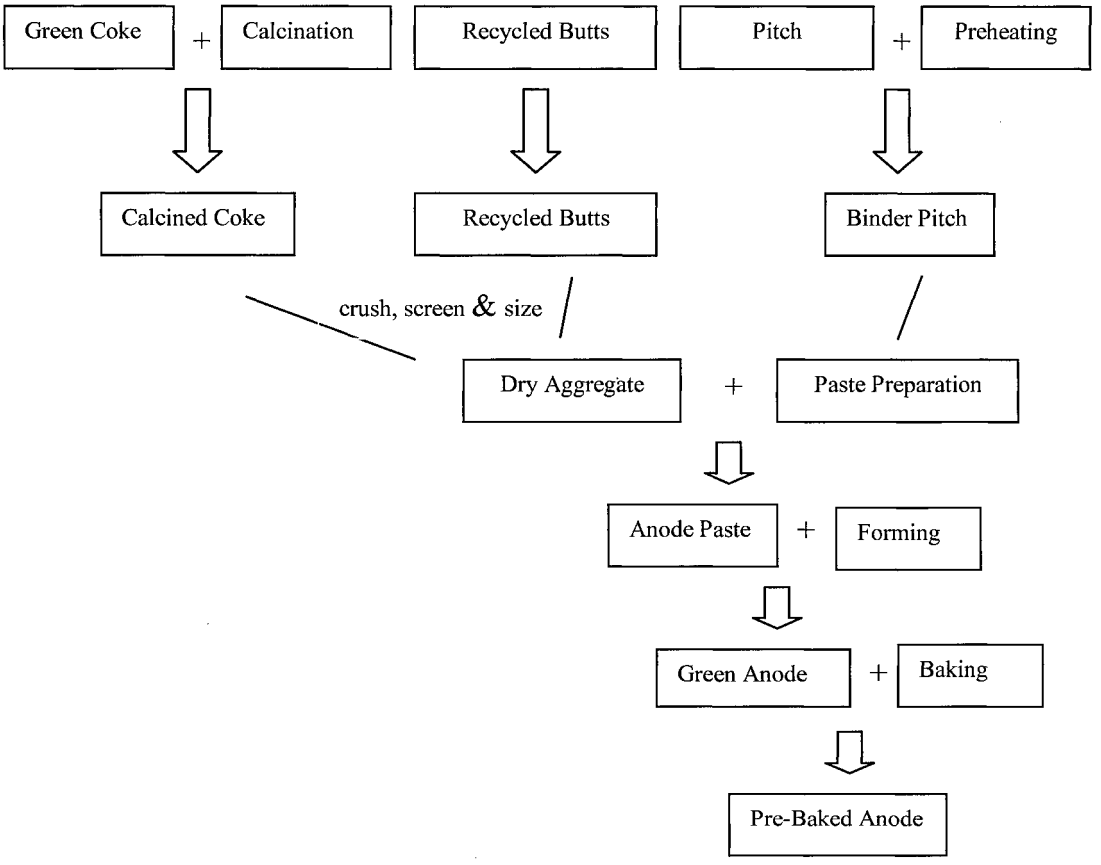

Figure 2.1 The pre-baked anode manufacturing process flow diagram of Chalco plant

2.2 Raw Materials

Carbon anodes are manufactured from three raw materials; petroleum coke, pitch, and recycled materials (butts, baked and green scrap). Coke and pitch are required in large quantities. These are stored and mostly prepared separately[12].

Petroleum coke

The properties of incoming coke depend on the material source. Coke quality is defined as the combination of chemical and physical properties that influence the

performance of anodes manufactured from it. Typical coke characteristics are shown in the Table 2.1[10] and Table 2.2 [11].

Table 2.1 Green coke properties (Worldwide)

Property	Method	Units	Range
Water Content	DIN 51304	%	0.0-0.2
Bulk Density	ISO DIS 10236	kg/dm^3	0.78-0.84
Grain Stability	ISO DIS 10142	%	75-90
Specific Electrical Resistance	ISO DIS 10143	$\mu\Omega m$	460-540
CO_2 Reactivity Loss (1000°C)	ISO N802	%	3-15
Air Reactivity 525°C	ISO N803	%/min	0.05-0.3
Ash Content	ISO 8005	%	0.10-0.20
Elements			
S	ISO N 837	%	0.5-3.5
V	ISO N 837	ppm	30-350
Ni	ISO N 837	ppm	50-220
Si	ISO N 837	ppm	50-250
Fe	ISO N 837	ppm	50-400
Al	ISO N 837	ppm	50-250
Na	ISO N 837	ppm	30-120
Ca	ISO N 837	ppm	20-100
Mg	ISO N 837	ppm	10-30

Table 2.2 Green coke properties (Chalco, Qinhai branch)

Property	Units	Range	Range
		Coke A	Coke B
Volatile Content	%	15.9	13.2
Ash Content	%	0.37	0.38
Elements S	%	1.62	0.46
V	ppm	437	< 20
Ni	ppm	156	464
Si	ppm	269	102
Fe	ppm	215	216
Na	ppm	33	104
Ti	ppm	13	8

Comparing the green coke properties of a worldwide typical coke (Table 2.1) and those of Chalco Qinhai branch's coke (Table 2.2) revealed that CO_2 reactivity and air reactivity measurements were not carried out in Qinhai branch.

Calcination:

Calcination is a thermal process in which green petroleum coke is heat-treated to 1200°C -1250°C. During calcination, moisture and volatile matter (such as hydrogen, methane, and tar) are removed. If not removed, these components might lead to cracking of anodes during the baking process due to shrinkage and coke devolatilisation. Cokes with significantly different volatile contents (quality and quantity), microstructure and/or

impurity levels must be calcined differently to obtain the optimal coke quality[4]. Coke undergoes structural changes during calcination, which improve properties such as crystalline size and real density[5]. Calcining is important to[12]:

1. achieve sufficient grain strength for handling;
2. minimise grain shrinkage;
3. ensure that the pore structure is accessible to binder pitch.

The most important calcining parameters for the petroleum coke quality are temperature, throughput, and residence time[13-14]. The final calcination temperature and residence time together determine the final real density of the calcined coke. The heating rate during calcination influences porosity as increased rates result in more rapid volatile evolution [15-17].

Pitch:

Pitch used for anode manufacturing is made from the distillation of high temperature coal tar petroleum that is a residue of petroleum refining industries [18]. Many researchers determined that the binder-matrix (mixture of dust and pitch) would be oxidized at first by air or CO_2 reaction. This is called selective oxidation[19]. Hence, optimizing the pitch content is important for pre-baked anode manufacturing[20-21]. Typical properties of pitch are shown in the Table 2.3[10] and Table 2.4[11].

Table 2.3 Pitch properties (Worldwide)

Property	Method	Units	Range
Water Content	ISO 5939	%	0.1-0.2
Softening point	DIN5 1920	°C	110-115
Density in water	ISO 6999	kg/dm^3	1.3-1.33
Coking Value	ISO 6998	%	56-60
Quinoline Insolubles	RDC 171	%	7-15
Toluene Insolubles	ISO 6379	%	26-34
Ash Content	ISO 8006	%	0.1-0.2
Elements			
S		%	0.3-30.6
Na		ppm	10-400
Ca		ppm	20-80
Si		ppm	50-200
Fe		ppm	50-300
Zn		ppm	100-500
Pb		ppm	100-300

Table 2.4 Pitch properties (Chinalco, Qinhai branch)

Property	Method	Units	Range
Softening point	DIN5 1920	°C	110
Volatile Content	-	%	54.8
Coking Value	ISO 6998	%	59
Quinoline Insolubles	RDC 171	%	14.9
Toluene Insolubles	ISO 6379	%	31.5
Ash Content	ISO 8006	%	0.67

Scrap:

Green and baked scrap is fed back into dry aggregates. Green scrap is generated from start-up/shutdown operations or changing process conditions within the plant. Green scrap is included in the anode recipe in quantities of up to 5%. Baked scrap such as rejected baked anodes is also often included in the recipe in small quantities and is processed with the butt component. Both green and baked scrap is usually stored in flat pots or bins[22-25].

Butts:

The butts are cleaned up from adhering impurities (bath material) and are then crushed, screened, sized, and mixed with the dry aggregate for use in anode production. The formulation for the new anode can contain up to around 30% of crushed butts. The quality of the butts can influence the quality of the anodes. The butts contain catalytic bath material hence adversely affect the reactivity of the new anodes[26-29].

2.3 Anode Baking Process

Anode baking process consist of four different parts: preheating, heating, forced cooling and natural cooling. Figure 2.2 shows the overview of Chalco's anode baking process[30-33].

Preheating

In the first 3 section of Figure 2.2, the flue gas temperature which varies from 200°C to 900°C increases the anode temperature from ambient temperature to around 550°C.

Between 200°C and 600°C, pitch volatiles start to evolve from the anode. These volatiles are drawn under the negative pressure into the flue (through the refractory wall openings) where the temperature is high enough to burn them.

Heating

In the next 3 sections, typically the gas temperature is raised up to around 1150°C by the combustion of fuel. Using the gas injectors which are installed on the burner ramps, the fuel can be injected into the flue. In this part, the anode temperature reaches a target temperature from the preheating temperature of around 550°C to the final temperature 1050°C in the Chalco plant. There is also a soaking period. During preheating and heating, the mechanical, physical, and chemical characteristics within the anode vary. The baked anode properties are affected significantly by the baking conditions.

Forced and Natural Cooling

In the next zone (3 sections after the heating section), a cooling fan seeks to provide enough oxygen for combustion in both the preheating and heating zones. And also the air has been preheated by the heat recovery from the refractory and anodes. Following these three sections, a cooling zone without heat recovery further lowers the temperature of anodes and the packing coke.

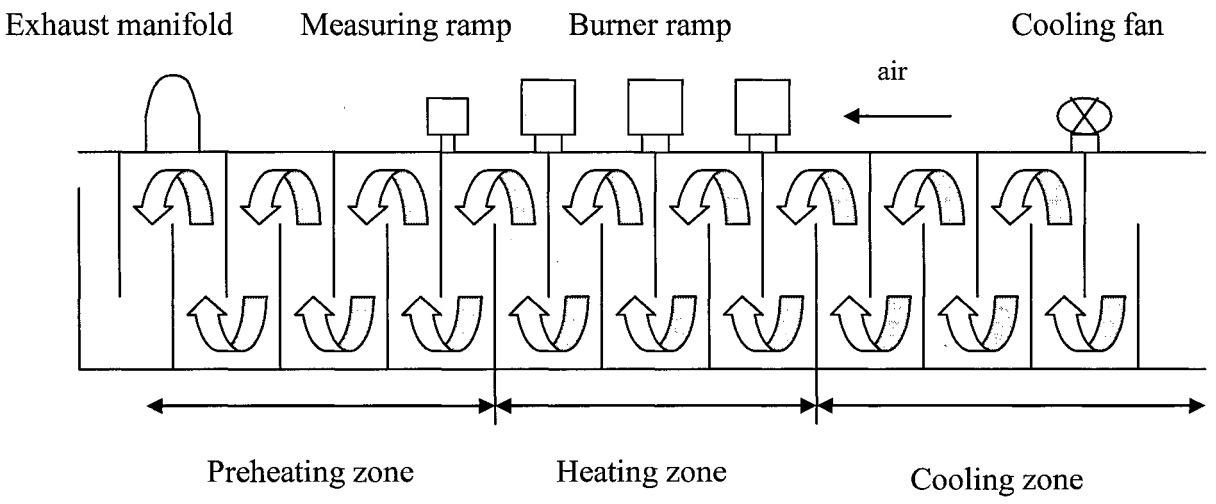

Figure 2.2 The baking process overview

During the baking process, the preheating zone is where the burning of the pitch volatiles takes place. Thus, utilizing the right timing of ignition temperature and the required oxygen content to maximize volatile combustion in the baking furnace became a popular research field in the recent years [34].

2.4 Anode baking optimization

The main baking conditions which relate to anode quality are anode heating rate, maximum baking temperature and soaking time[35-37].

The heating rate is related to anode flexural strength and electrical resistivity. If anodes are heated up too fast, it will cause those anodes to crack. The micro-cracks may start inside the anode gradually during the baking process, and then series of cracks forming from the internal part of the anode to the surface might yield the splitting of anode.

The maximum baking temperature affects the CO_2 reactivity, air reactivity and thermal conductivity. Higher maximum temperatures decrease CO_2 reactivity, air reactivity and increase thermal conductivity. In most cases, excessive thermal conductivity might cause air burn at the anode top. Thus, the control of maximum baking temperature is important for the optimization of the anode quality and the prevention of anode overbaking.

Soaking process is the last step of anode heat treatment. The major target of soaking is to heat the anodes which are placed at the different positions evenly. The longer soaking times result in better uniformity of anode properties.

2.5 Pitch volatiles

Typically, in the carbon plant, the temperature of anode baking is always less than the temperature of coke calcination. The volatiles released from the anodes during the baking process come from the pitch, thus called pitch volatiles. There are two parts of pitch volatiles, non-condensable gas and condensable gas. Three main components of these gases are hydrogen and methane, which represent the non-condensable part, and tar, which represents the condensable part. Tar also includes polycyclic aromatic hydrocarbons (PAH). PAHs with six or less combined aromatic rings are known as 'small PAHs', and those containing more than six aromatic rings are called 'large PAHs'. The PAHs of pitch volatiles are mainly of 'small' PAHs type. [38-39]. The composition of the tar component was not analyzed in this study.

According to the energy balance, the heat the pitch combustion could produce actually is more than that needed for anode baking energy consumption. In other word, increasing the pitch volatiles combustion not only reduces the costly fuel consumption down to a minimum, but also achieves clean production. [40-41].

Chapter 3

Experimental

3.1 Introduction

In this project, first an investigation has been carried out on raw materials in order to optimize the anode recipe. This part involves a review of production process in order to determine the problem points in the plant followed by the anode production with different particle size distributions. The relationship between the anode formulations and anode properties (permeability, air reactivity, and CO_2 reactivity) were studied. This part was carried out at the Chalco plant in Guizhou, China. Then, a study on kinetics of anode baking is carried out at UQAC. In this part, the anode formulation that yielded the best properties in the previous part was chosen to simulate the baking process in the laboratory. The devolatilisation (tar, H_2, and CH_4) kinetics were investigated. Again, the anode properties were measured after baking the anodes under different conditions. This serves to determine the conditions that lead not only to improved anode quality but also more efficient utilisation of released volatiles to reduce the energy consumption. A schematic diagram of the experimental plan is shown in Figure 3.1. Via repeated trials following the experimental procedure, different production formulations, conditions, and parameters were tested and improved. The results were transferred to the plant for implementation in the plant operation.

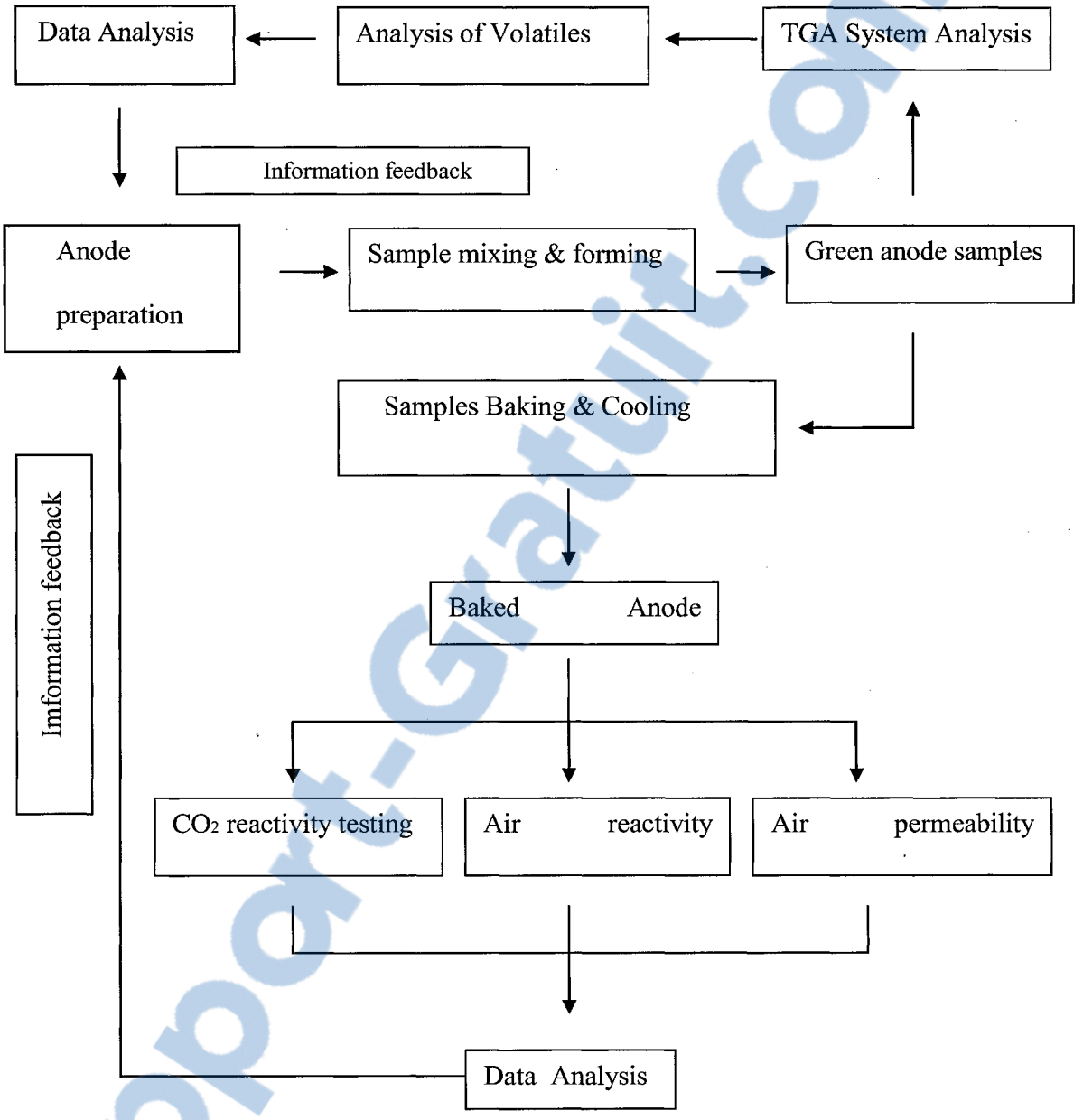

Figure 3.1 A schematic diagram of the experimental plan

3.2 Experimental Set-up

3.2.1 Equipment for anode preparation in laboratory:

Bench Scale Unit for Green Anode Preparation (Fig. 3.2,)

The bench scale unit (R&D Carbon RDC 161) for green anode preparation consists of a kneader and a press. Anode formulation studies require the adaptation of the pitch level as well as the adjustment of the particle size distribution, which necessitate a large number of tests[42-43]. Table 3.1 shows the specifications of this unit.

Table 3.1 Specifications of of green anode preparation bench scale unit

Power Supply	9 kW
Electrical Connection	3 x 380 V, 50/60 Hz
Dimensions (LxWxH)	130 x 110 x 213 cm
Weight	1100 kg

Anode Baking Furnace (Fig. 3.3)

The R&D Carbon RDC-166 anode baking furnace was used for the baking of the green anodes. The furnace simulates the industrial process. The green anodes are placed in the furnace and surrounded by packing coke. These trials serve to maintain the quality raw material selection and to ensure the quality control of pre-baked anodes[44-45]. Table 3.2 gives the specifications of anode baking furnace.

Table 3.2 The specifications of baking furnace

Power Supply	5.5 kW
Electrical Connection	3 x 380 V, 50/60 Hz
Dimensions (LxWxH)	120 x 80 x 179 cm
Weight	300 kg

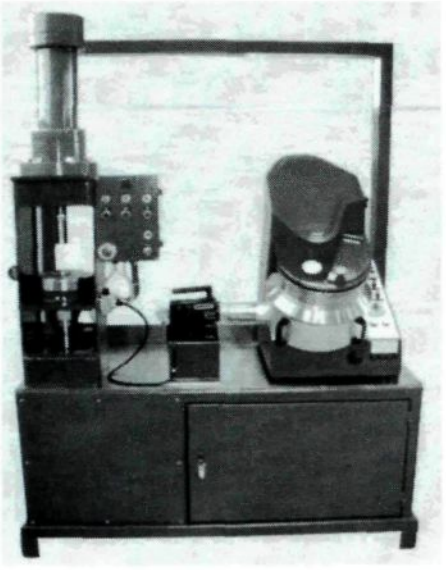

Figure 3.2 Green anode preparation

Figure 3.3 Anode baking furnace

3.2.2 Equipment for anode property measurement

Reactivity of Anodes (Fig. 3.4)

Carbon reacts with carbon dioxide according to the endothermic reaction:

$$CO_2 + C = 2CO \qquad (3.1)$$

This reaction always takes place in the electrolysis cell. In aluminum production where electrolytic cells operate at 950-960°C (1745-1760°F), carbon dioxide, generated at the anode interface by electrochemical oxidation, can attack the carbon anode via this reaction. The total weight loss which is equal to the difference between the original sample weight and final weight after reacting with CO_2 is the CO_2 reactivity percentage (%) residue[46-47]. Table 3.3 shows the standard used and the specifications of the equipment.

Table 3.3 The specifications of CO_2 reactivity test

ISO Method	12988-1
Power Supply	2.0 kW / 6.0 kW
Electrical Connection	2Lx380 V / 3x380 V - 50/60 Hz
Gas Supply	CO_2 ; adjusted to 2 bar on manometer
Gas Connection	Tube: External Diameter 6 mm, Internal Diameter 4 mm, must withstand 10 bar
Gas Flow Rate	200 l/h, min. 3 bar
Gas Quality	CO_2 better than 99,5%
Furnace Heat-up Time	Appr. 2 hours from room temperature to 960 Deg C
Furnace Temperature (during test)	960 °C
Vapours Emitted	CO (Carbon Monoxide)
Test Time (excl. sample preparation)	9.5 h for 2 samples in 1 furnace
Number of Samples/Test	two
Sample Length	60 mm
Sample Diameter	50 mm

Air Reactivity of anode (Fig. 3.5)

During aluminum electrolysis, the air-burn causes the anode consumption and increases the temperature of the upper surface. Following two reactions are possible since the anode upper surface temperature is generally between 550°C and 650°C:

$$C + O_2 = CO_2 \quad (3.2)$$

$$2C + O_2 = 2CO \quad (3.3)$$

The air reactivity can be measured by using the R&D Carbon RDC 151 apparatus. After the reactivity tests, the samples are cooled from 550°C to 400°C with cooling rate of 15°C /h. After cooling and weighing, the samples are mechanically tumbled with steel balls in a separate piece of equipment (R&D Carbon RDC-181, tumbling apparatus) to remove any loosely-bound particles. The total weight loss equals the difference between the original and final sample weight and is presented as the air reactivity percentage (%) residue[48-49]. Table 3.4 shows the standard used and the specifications of the equipment.

Air Permeability (Fig. 3.6)

The gas permeability of the material has a great influence on both CO_2 and air reactivities. A high permeability leads to increased reactivity since CO_2 or air can penetrate into the anode which increases the anode consumption even further. The gas permeability of anodes were measured using the R&D Carbon RDC-145 apparatus. The permeability is determined by measuring the time that a gas needs to pass through a sample in order to refill a partly evacuated system. The sample has a disc shape with a diameter of 50 mm and

a length of 20 mm [50-51]. Table 3.5 shows the standard used and the specifications of the equipment.

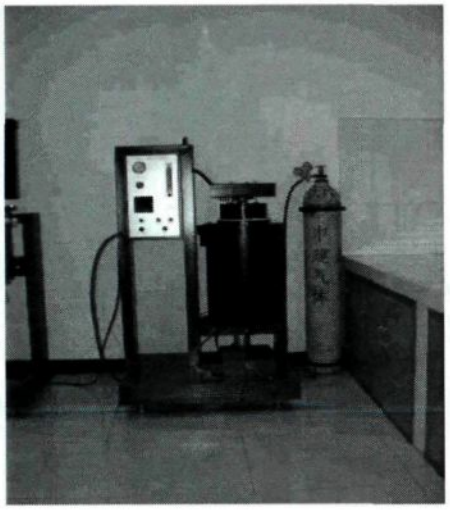

Figure 3.4 CO_2 reactivity of anodes

Figure 3.5 Air reactivity of anodes

Figure 3.6 Air permeability

Table 3.4 The conditions of air reactivity test

ISO Method	12988-2
Power Supply	1.1 kW / 3.3 kW
Electrical Connection	2 L x 380V / 3 x 380 V - 50/60 Hz
Gas Supply	Air ; set to 2 bar on manometer
Gas Flow Rate	200 l/h min. 4 bar
Gas Quality	Air, N_2 : 78%, O_2 : 21%, Ar : 1%, H_2O < 150 mg / Nm3, free of oil
Vapours Emitted	CO_2
Test Time (excl. sample preparation)	11.5 h for 1 sample
Number of Samples/Test	two
Sample Length	60 mm
Sample Diameter	50 mm

Table 3.5 The specifications of air permeability test

ISO Method	15906
Power Supply	0.5 kW
Electrical Connection	220 V, 50/60 Hz
Air Pressure Setting (1)	2 bar
Test Time (excl. sample preparation)	Appr. 2 minutes
Number of Samples/Test	one
Sample Length	20 mm
Sample Diameter	50 mm

3.2.2 Equipment for Devolatilisation Kinetics Measurement :

Thermogravimetric Analyser (TGA) Coupled with Gas Chromatograph (GC)

Figures 3.7 to 3.11 show different parts of the system, and Figure 3.12 shows the flow diagram.

Thermogravimetric Analyser (TGA)

The sample was tied by metal wires and then suspended from a balance for measuring the weight loss of anode sample during baking. The nitrogen gas was used as the carrier gas and protection gas for both TGA and gas chromatograph. The carrier gas nitrogen enters the furnace from the bottom. Rotameters R23 and R13 control the gas flowrate. The carrier gas flowrate is not only important for the success of anode baking test but also important for the calculation of the amount of each volatile. During baking, part of the gas with a known flowrate was suctioned for analysis with GC. Both the main outlet gas and GC sampling gas was passed through a cold trap in order to separate the tar. In the cold trap, cold water with a temperature less than 4°C was recirculated. This prevents the blockage of the connection tubes and rotameters, thus, protects both TGA and GC system efficiently and make this system work well.

It can be seen from the figure 3.12 that the gases for analysis (red line) pass through the condensable tank, glass wool filter and the rotameters R1, R2 and R3. An automatic controller ensures the injection of gas for analysis. At that time, the valve Q3 closes, then Q1 and Q2 open automatically and the sampling gas trapped in the injection coil flows in to

the column. After GC injection, Q1 and Q3 close, Q2 opens, the gas goes out directly due to suction. The rest of the outlet gas is pumped out by Pump 1A and Pump 1B continuously.

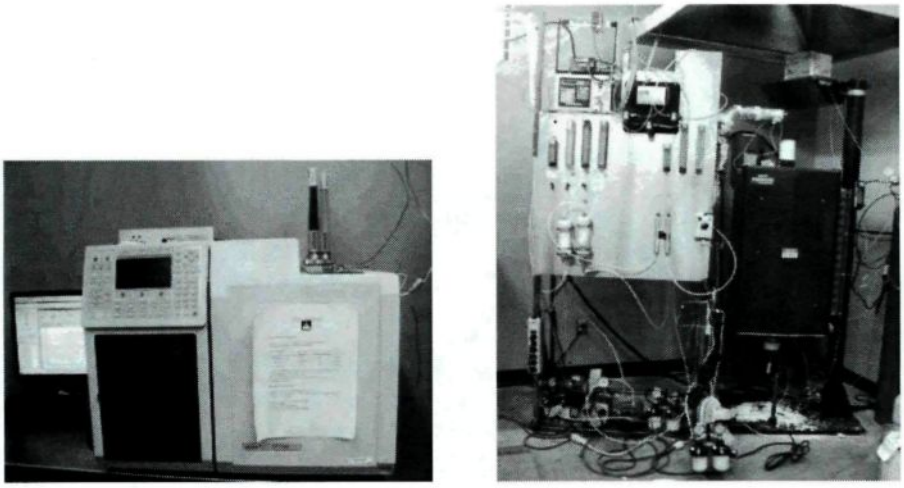

Figure 3.7 Coupled TGA-GC analyzer

Figure 3.8 TGA controller

Figure 3.9 Cold trap

Figure 3.10 Anode sample

Figure 3.11 Carrier gas cylinders

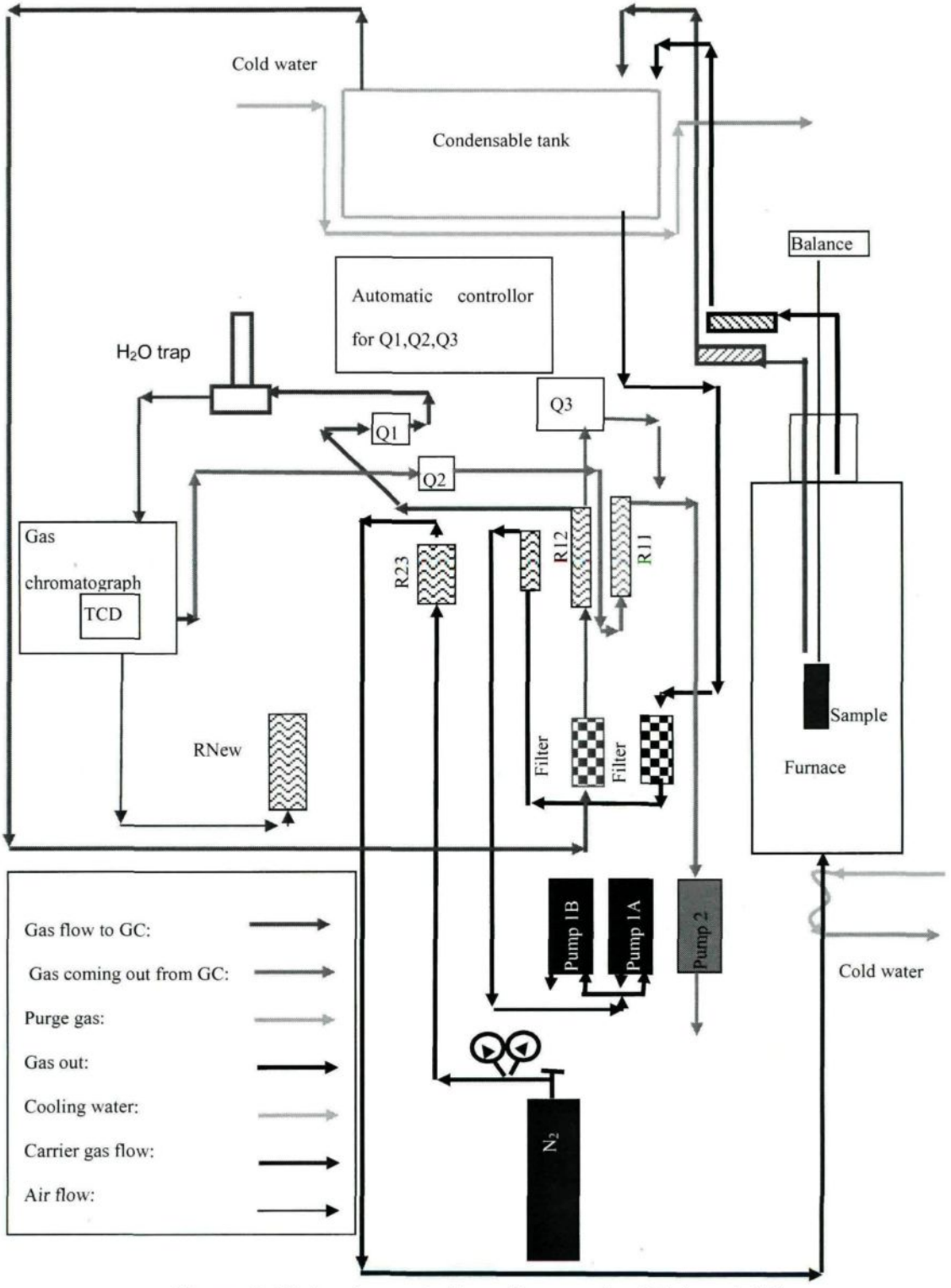

Figure 3.12 A schematic flow diagram for TGA and GC

Gas Chromatograph (GC)

The nitrogen gas was used as the carrier gas for the GC (Varian 3800) analysis. Compressed air was used for the injection valve operation. A known volume of sample gas was stored in the injection cycle and injected into the column with the help of this valve. An injector type 1061 was used. The column was packed with 13X molecular sieve. This type of column can separate hydrogen and methane well. After the injection, the column adsorbs all the gases, and desorbs each gas separately. GC was equipped with thermal conductivity detector. The thermal conductivities of the sample gas mixture were compared with that of the carrier gas which was flowing on the reference side of the detector. The Wheatstone bridge arrangement was used for the TCD measurements[51-53]. Through the calibration of thermal conductivity vs. the gas concentration for each gas, their concentrations were determined from the areas of the desorption peaks. Table 3.6 shows the details of GC conditions for the gases analysis.

An example of hydrogen and methane peaks obtained during the experiments is displayed in Figure 3.13. This figure shows that H_2 and CH_4 peaks were separated quite well during the gas chromatograph test. The peak of methane always appeared after that of hydrogen.

Table 3.6 The GC analysis conditions for hydrogen and methane

Gas Chromatography : Varian 3800	
Detector : TCD	
Column : Molecular sieve 13X	
Analysis condition	
Column temperature	60°C
Injector temperature	70°C
Detector temperature	120°C
Filament temperature	180°C
Volumn of injector	1 mL
Carrier gas	Nitrogen
Flow rate of carrier gas	20 ml/L
Injector	Continuous injection

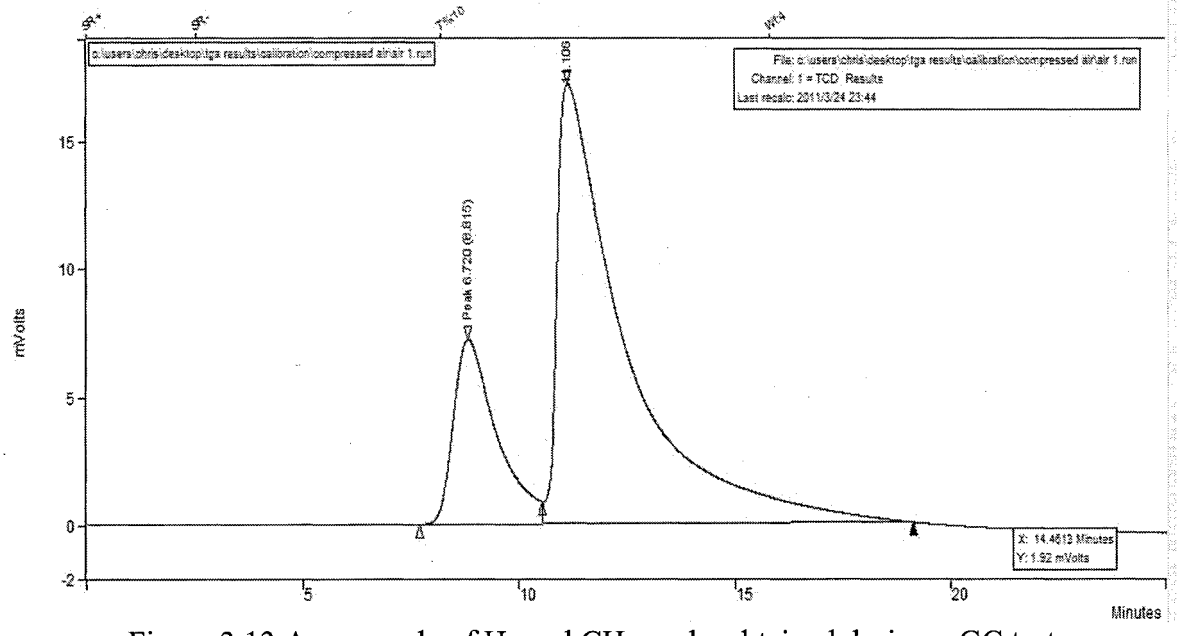

Figure 3.13 An example of H_2 and CH_4 peaks obtained during a GC test

Figure 3.14 and Figure 3.15 show the calibration curves of hydrogen and methane. They both gave high correlation factors (R^2).

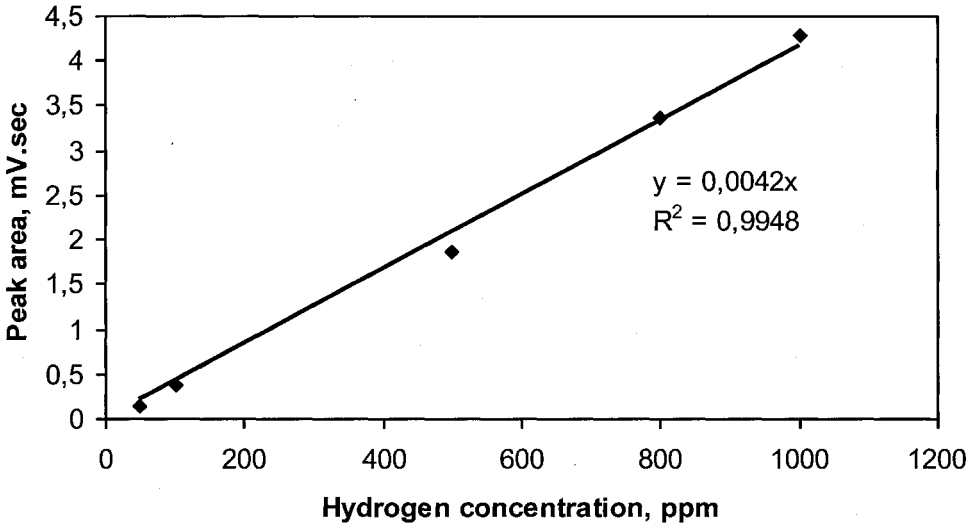

Figure 3.14 The calibration curve of hydrogen

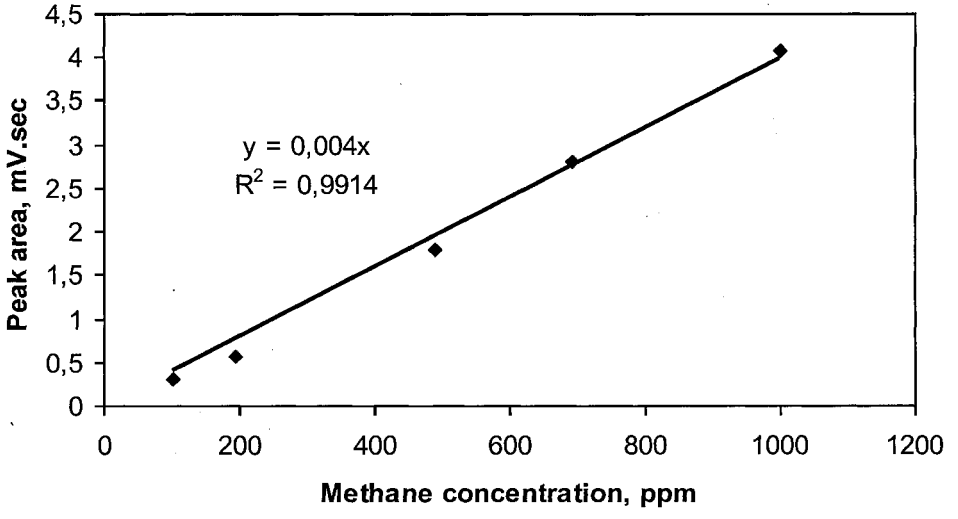

Figure 3.15 The calibration curve of methane

3.3 Methodology

3.3.1 Characterization and analysis of raw material

The raw materials used in anode production were tested for the trace elements content using Chinese Nonferrous Metals Industry Testing Standards YS/T 587[30]. These raw materials were analyzed using SEM-EDS. Samples were treated and polished using ASTM D 2797[32].

3.3.2 Anode formulation experiments

The anode formulation experiments were separated into two groups. The small particle group for which the maximum particle size was less than 12mm was marked group A. The big particle group which had the particle sizes larger than 12mm was marked group B. In each group, different recipes were tested to determine the effect of each size fraction. Finally, a recipe which resulted in best anode properties (air reactivity, CO_2 reactivity, and air permeability) [32] among those tested was chosen for further analysis.

3.3.3 Thermogravimetric experiments and volatiles analysis

Small anode samples were prepared based on the best recipe obtained from the anode formulation experiment with the raw materials available in the Guizhou province of China using the same procedure followed by the industry. These anodes were baked in a thermogravimetric analyzer. The effects of the following baking parameters on the anode properties (CO_2 reactivity, air reactivity, air permeability) were studied and correlated with anode preparation conditions.

- Heating rate
- Soaking time
- Baking temperature

Anode quality (properties) were also correlated with anode preparation conditions. Gas devolatilisation analysis was carried out. Kinetic parameters were determined for differen baking conditions.

3.4 Model for devolatilization kinetics

During the baking of green anodes, tar, CH_4, and H_2 are produced due to the cracking of pitch volatiles. The kinetics of formation of tar, CH_4, and H_2 can be determined using the thermogravimetric analysis coupled with the gas chromatography. In this work, the kinetic parameters were calculated using the model developed by Kocaefe et al.[16] assuming that H_2, CH_4, and tar form. It was assumed that devolatilisation of each component follows nth order rate equation of the form:

$$\frac{dX_i}{dt} = k_i C_0^{(n-1)}(1-X_i)^n \qquad (3.4)$$

X_i: conversion of component i (i denotes H_2, CH_4 or tar)

n : order of reaction

k_i: rate constant for gas i ($s^{-1}\cdot concentration^{1-n}$)

It is further assumed that the rate of devolatilization is dependent on the temperature and follows the Arhenius law.

Thus k can be expressed as:

$$k_i = k_{i0} \exp(-E_i / RT) \tag{3.5}$$

k_{i0}: Pre-exponential factor for gas i ($s^{-1} \cdot concentration^{1-n}$)

E: activation energy [J/mol]

R: gas constant [8.314 J/mol K]

T: Temperature [K]

In this work, the activation energy, rate constant, and the order of the reaction for all the formation reactions were determined by the differential method.

3.4.1 Determination of kinetic parameters

Here the basis of calculation for the determination of kinetic parameters for the formation of H_2, CH_4, and tar is described. As there is no gas chromatography data available for tar, the instantaneous weight loss due to this component was found from the difference between the instantaneous total weight loss and the instantaneous weight loss due to H_2, CH_4 calculated using the GC data. After the calculation of the instantaneous rate of tar, the method of calculation of its kinetic constants is the same as those of H_2 and CH_4. Below, the general method for the calculation of kinetic parametrs is explained.

Using the chain rule given below (Equation 3.6),

$$\frac{dX_i}{dt} = \left(\frac{dX_i}{dT}\right)\left(\frac{dT}{dt}\right) = \left(\frac{dX_i}{dT}\right) h \tag{3.6}$$

combining the Equations 3.4, 3.5 and 3.6, defining the heating rate (h=dT/dt), and taking the logarithms of both sides give:

$$\ln\left(\frac{dX_i/dt}{(1-X_i)^n}\right) = -\frac{E_i}{RT} + \ln\left(\frac{k_{i0,app}}{h}\right) \tag{3.7}$$

where apparent pre-exponential factor is defined as

$$k_{i0,app} = k_{i0} C_0^{(n-1)} \tag{3.8}$$

The following Figure 3.16 gives an example of tar kinetic parameters determination by plotting ln (dX_i/dT / $(1-X_i)^n$) vs. 1/T (see Equation 3.7). The best line is determined. Data were plotted using different n values and the one that gives the best linear relationship (best R^2, correlation coefficient) was taken as the solution.

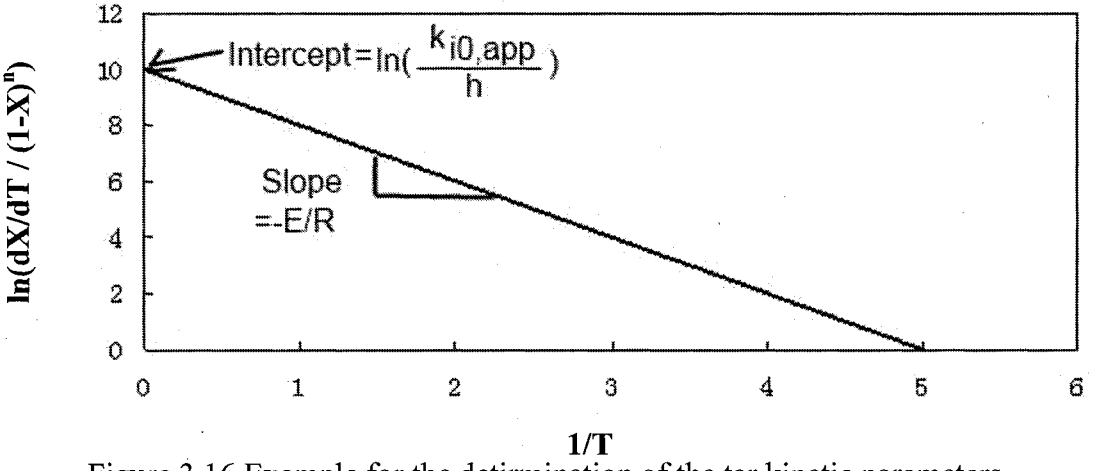

Figure 3.16 Example for the detirmination of the tar kinetic parameters

3.4.2 Determination of conversion (X) for each gas component

A part of the outlet gas was withdrawn for analysis. Then, its methane and hydrogen content was analysed using a gas chromatograph equipped with a thermal conductivity detector. The detector response was calibrated for methane, hydrogen, and oxygen using calibration gases of known concentrations. Data on oxygen was used to detect if there was any air leak on the line and correct the gas concentration if necessary.

1. Calibration: The objective of calibration of gas chromatograph response is to find the relationship between the peak area and its corresponding concentration of a given gas component. The area under the peak obtained was measured with the software of the gas chromatograph. Thus, dividing the known value of concentration (ppm) by the area obtained using GC, the concentration as 'ppm per unit area (PPMA)' for the particular component can be calculated. Using different concentrations, the calibration curve was prepared to use later on in the TGA-GC measurements.

2. Calculation of concentration of a component:

The concentration of the component in ppm is equal to area of peak obtained by GC multiplied by PPMA for the component. However, the gas in the TGA always contains some air, i.e., air slightly dilutes the concentration of the component so the calculated ppm of the component is always less than the exact ppm on air-free basis. That is why the dilution ratio has to be determined and the correction has to be made.

3. Calculation of the instantaneous mass flowrate of the component:

By definition of ppm,

Y ppm of a gas = mole of the gas / 10^6 mole of total (3.9)

For an ideal gas, 1 mole of the gas occupies a volume of 22400 ml.

The instantaneous mass flow rate of gas in g/min =

$$Y*M*(\text{total flowrate in ml/min})/10^6*22400 \quad (3.10)$$

where M is the molecular weight of the gas.

4. Instantaneous rate of total weight loss in g/min:

To determine the instantaneous rate of total weight loss in g/min, the weight loss vs. time curve is differentiated numerically. The slope of the curve at each time gives the instantaneous total weight loss in g/min.

5. Presentation of the instantaneous total weight loss per 100 g of anode sample:

As all the calculations are dependent on the weight of the sample, the calculation has to be made independent of the initial weight of the sample. Therefore, the data is represented on the basis of 100 g of sample. Thus, the instantaneous amount of gas in g/min per 100 g of sample is expressed as:

Instantaneous total weight loss of gas (g/100g of sample) =

(Instantaneous total weight loss, g/min) * (100/initial weight of sample, g) (3.11)

6. The instantaneous methane and hydrogen release data are already available from the GC analysis. The difference between the total and the sum of hydrogen and methane gives the instantaneous tar release data.

7. Calculation of cumulative data per 100 g of anode sample:

The integration of the curve representing the instantaneous amount of gas component vs. time (the area under the curve) gives the cumulative data for all three components.

8. Calculation of conversion for the component:

The conversion is calculated by dividing the cumulative weight loss of a gas component at a particular time by total amount of weight loss for that component.

Thus the conversion for a species at a particular time is given by:

Conversion (t) = Cumulative weight loss for a species (t) / Cumulative weight loss for that species (3.12)

Chapter 4

Characterization and analysis of raw material

4.1 Introduction

For optimizing the anode properties (air permeability, air reactivity, and CO_2 reactivity), first it was necessary to do an investigation in the Chalco plant in order to understand their anode production process and their operation. This was necessary for assessing the key points that could be improved as soon as possible and aligning the research project along with the results of this assessment. The results of the sampling and testing of the raw materials (pitch, dry aggregate which consists of coke, recycled butt and anodes) indicate which parts of the process need attention and help better focus the work. The anode quality optimization was based on a large number of single-factor as well as orthogonal experiments in order to adjust the specific production processes at the laboratory scale. The different production formulations, conditions, and parameters were tested repeatedly. Finally, the results of this project was implemented in the plant operation after the necessary technology transfer.

In this chapter, a review of the anode production process, from the raw material storage yard, raw material transportation lines, calcination kilns, calcined coke cooling kilns, the green mill to the forming system was carried out. Each part had been visited, pictures and samples were taken in order to determine which part needs the most attention. The results are summarized in the following section.

4.2 Results

4.2.1 Investigation of green anode manufacting process

The coke is transported to the plant by train. At first, it is piled in the outside yard, waiting to be transported by trucks and scrapers into the storage. Then, it is passed through a crush line called a "pre-crush" process to adjust the coke particle size before the raw material is fed into the calcination kilns. (see Figures 4.1 to 4.4).

Figure 4.1 Coke pile in the outside yard

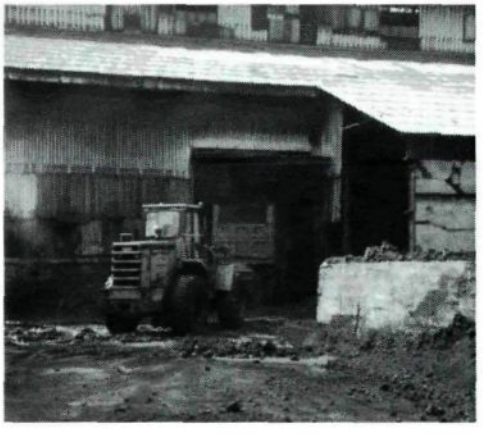

Figure 4.2 Coke transportation

Figure 4.3 The "pre-crush" unit

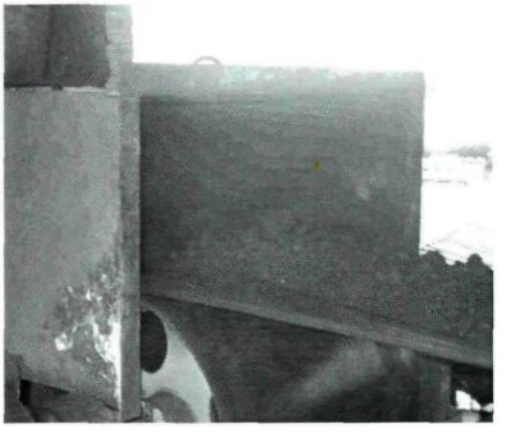

Figure 4.4 Coke conveyor and feeding hole

After the "pre-crush" process, the "pre-crushed" coke is moved into the calcination kilns by a conveyor.

Calcination

During the calcinations process, the green coke is calcined in large kilns up to 1200°C with the gas temperature around 1500°C. In the plant, the kiln is divided into three parts for the control of the calcination temperature. The part which is connected to the feeding bin is called the "tail", the temperature of this part is the lowest. The middle of the kiln is called the "body" at the highest temperature. The exit of the kiln is called the "head" at the medium temperature. Thus, the calcination takes place mainly in the "body" section. Afterwards, the calcined coke is fed into a cooling kiln to lower the temperature of the coke (see Figures 4.5 and 4.6).

Figure 4.5 Calcination kiln

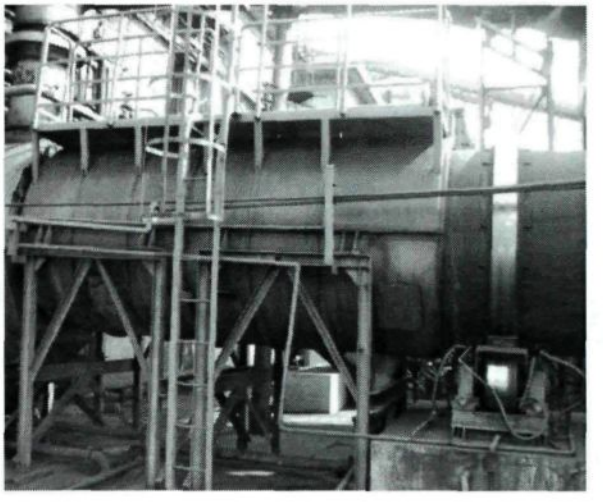

Figure 4.6 Cooling kiln

Green Mill and Forming

Before mixing and forming, all the raw materials are crushed, screened, and sized according to predetermined size distribution and added together to form a dry aggregate. This aggregate is then preheated to around 165°C and mixed with 15 wt% liquid pitch that is preheated to a temperature between 150°C and 180°C. Then, the anode paste is formed into a green anode block by the vibratory compaction (Figure 4.7).

Figure 4.7 Vibratory compaction unit

Recycled Anode Clean-Up

The butts which are fed as part of dry aggregate are cleaned by removing the adhering impurities (bath material, see Figures 4.8 and 4.9) and are then crushed, screened, sized to two fractions (coarse 3~12mm and fine < 3mm), and transported into the aggregate for anode production.

Figure 4.8 Recycled anode butts

Figure 4.9 Automatic shoot penning equipment for butts clean-up

In the new anode recipe, a recycled anode can be between 20% to 25%. The quality of the butts can influence the quality of anodes. The butts contain catalytic bath material hence adversely affecting the anode reactivity.

After visiting all the production units, the experiments were started in the laboratory. There were a number of findings which pointed out some of the challenges in the production process during the review; and these are summarized in the following part.

4.2.2 Preliminary Experiments:

At first, all the samples which were taken from different parts of the anode production process were tested and analyzed for trace elements using SEM methods.

Trace Elements Testing

The trace element testing method is based on YS/T 587- Chinese Nonferrous Metals Industry Testing Standards. Tables 4.1 to 4.3 summarize the results.

Table 4.1 Water and S contents of the cokes

	Water Content (%) using standard YS/T 587 2006	S content (%) using standard YS/T 587.4 2006
1# Green Coke	1.00	2.10
2# Green Coke	0.54	2.12
1# Calcined Coke	0.12	1.70
2# Calcined Coke	0.13	1.73
3# Calcined Coke	0.13	1.65
4# Calcined Coke	0.14	1.70
0# Calcined Coke	0.04	1.30
Pitch	-	0.30

Table 4.2 Trace elements of raw materials

Sample	Units	Fe	Ca	V	Si	Na
1#Calcined coke	ppm	1160	1590	150	11600	350
2#Calcined coke	ppm	1520	1690	180	4100	430
3#Calcined coke	ppm	700	1630	120	13500	260
4#Calcined coke	ppm	720	480	170	2500	320
Green coke	ppm	300	210	170	4600	138
Pitch	ppm	450	640	60	5600	

Table 4.3 Trace elements content of sized cokes and paste

Sample	Units	Fe	Ca	V	Si	Na
Coarse	ppm	525	2490	333	7860	-
Fine	ppm	491	2211	260	3200	-
Recycled coarse	ppm	4352	1703	145	2300	1320
Recycled fine	ppm	1457	1681	350	7350	2796
Dust	ppm	701	1842	108	5380	-
Anode paste	ppm	598	1913	235	4380	-

Among the results, especially four elements reflect the raw materials' characteristics used by Chalco. The vanadium content is normal, but the Fe, Ca, Si, and Na contents are too high and they affect seriously the properties of the anode reactivity. The SEM analysis was carried out to investigate the morphology of the metal impurities. The results of SEM analysis is presented below.

SEM Analysis

The samples of calcinated cokes, anode paste, baked anodes, and recycled anodes were treated and polished using ASTM standard D 2797. The findings of SEM and EDS analysis are explained below.

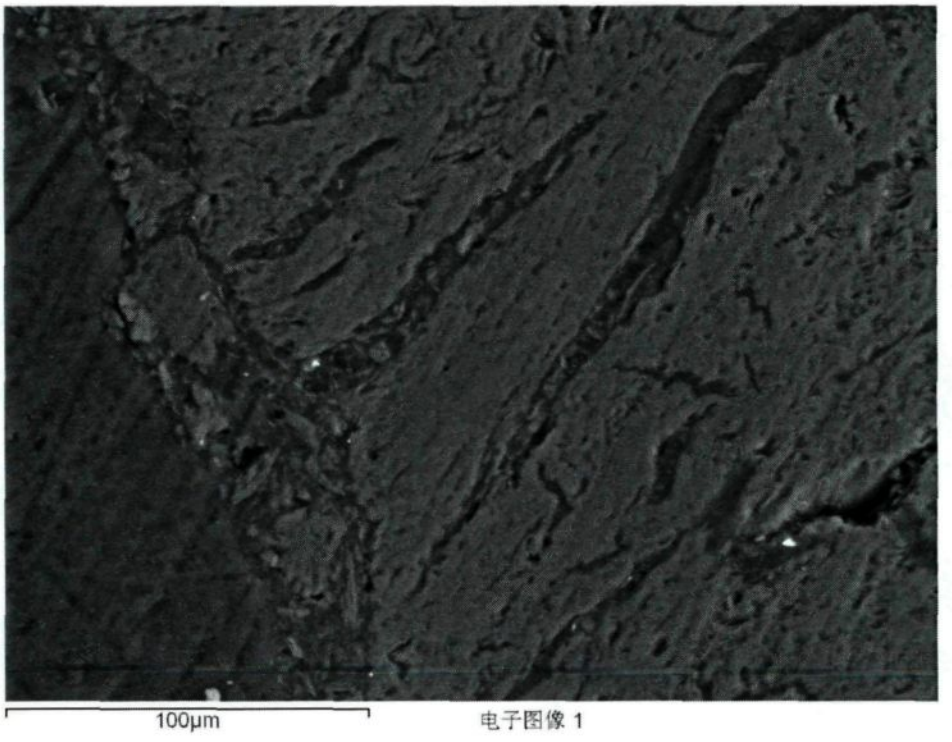

Figure 4.10 Image of anode paste

The Figure 4.10 shows the wetting and penetration behavior of the binder-matrix (mixture of dust and pitch). At optimum conditions, the pitch/fines binder matrix penetrates the fissures and pores of the coarse petroleum coke particles and thinly coats these particles[54-55].

SEM-EDS image showed the presence of La and Ce. Figures 4.11 to 4.18 show these elements in different materials. Arrows shown on SEM micrographs of the figures below points to the positions of these rare earth elements, La and Ce, which were found in the calcined coke A, recycled butt A, and anode A. Anode A has coke particle sizes less than 12mm as explained in Chapter 3 whereas Anode B contains larger coke particles.

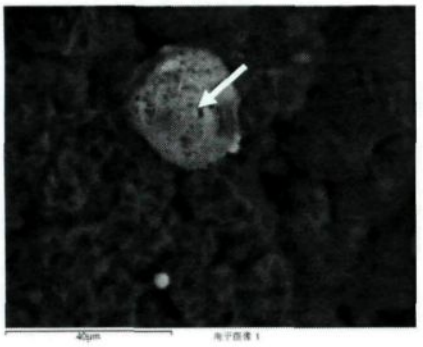

Figure 4.11. SEM images of coke A

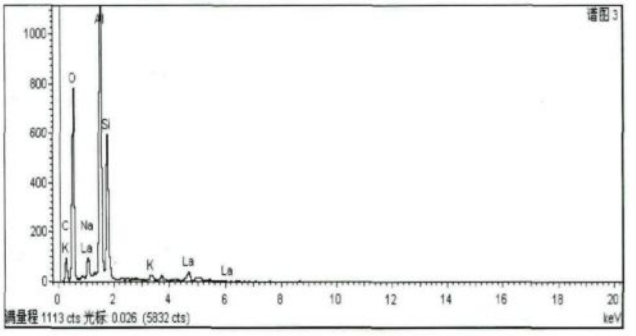

Figure 4.12. EDS patterns of the La element in coke A

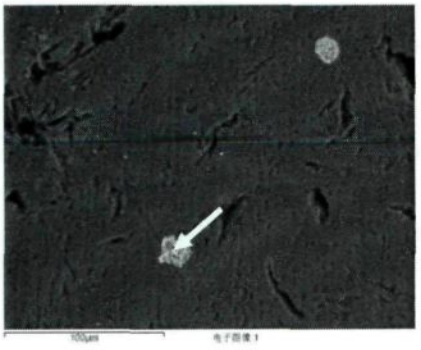

Figure 4.13.SEM images of carbone anode A

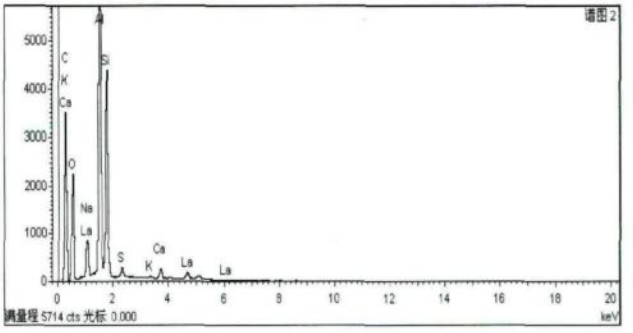

Figure 4.14. EDS patterns of the La element in carbone anode A

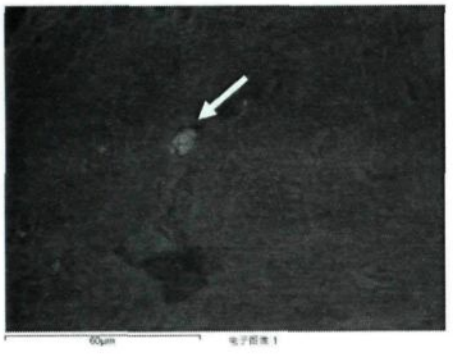

Figure 4.15. SEM images of carbone anode A

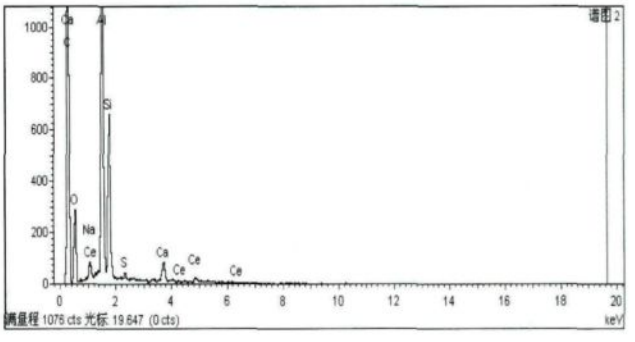

Figure 4.16. EDS patterns of the Ce element in carbon anode A

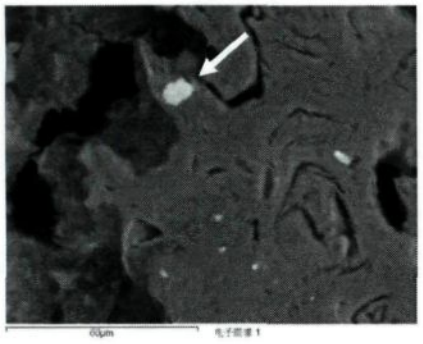

Figure 4.17.SEM images of recycled butt A

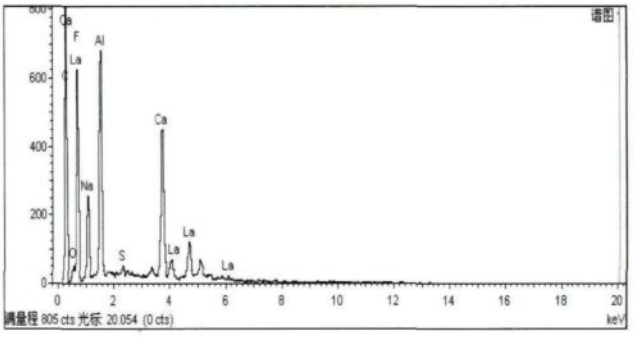

Figure 4.18. EDS patterns of the La element in recycled butt A

Figures 4.12, 4.14, 4.16, 4.18 show the difference in La and Ce quantities present in raw materials and anodes. Figure 4.11 illustrates that calcined coke containing La has a rough surface with pores and cracks. The structure of La particles is granular. Figures 4.14 and 4.16 show the presence of La and Ce in the anode samples. Both of elements seem to be flat and stuck on the surface of the sample. Figure 4.18 shows the presence of La in the recycled butt. The structure of La particle is flat and stuck on the surface of recycled butt, similar to the anode sample. Figures 4.11, 4.13, 4.15, 4.17 show the distribution of the elements at the point where arrows are pointed. As it can be seen from these figures, the La and Ce coexist with the Al, Na and Si. From the analysis, it can be said that the rare earth elements might exist in the green coke as well as in anode butts. During the anode manufacturing process, these elements are mixed into the anode paste.

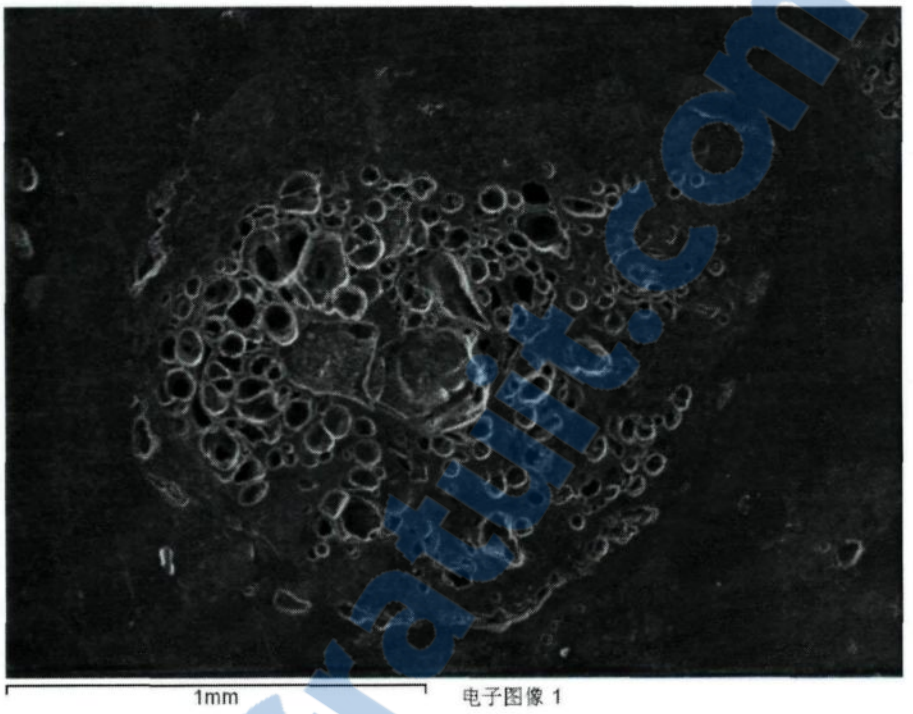

Figure 4.19 Image of calcined coke

Figure 4.19 show that there are large amounts of pores inside the calcined coke due to release of volatiles during calcination. The analysis showed that these types of cokes are found in the anode paste. They may increase the porosity and air permeability of anode. Thus, the small particle size distribution anode (Anode A) was tested in the anode formulation experiments to increase the contact area of coke and pitch[56] and to decrease the anode porosity.

4.3 Discussion of results

Three key results found at the end of the first series of experiments are as follows:

1. The impurities Fe, Ca, Si, Na are mainly trace elements in raw materials, intermediates and baked anodes, and these elements can greatly affect the anode reactivity. Thus, it

was suggested to the plant that these four elements are traced and controlled in the future production. However, the following question remains: how to decrease the contamination of raw materials and anodes during the production process? This problem will be addressed in the conclusions part.

2. The formulation of the anode paste was tested and adjusted and presented in the next chapter. The attention was given especially to the adjustment of the recycled anode content in the recipe because most of Na and Fe come from the recycled anode during the paste preparation.

3. The rare earth elements La and Ce were discovered in the raw materials, baked anodes, and recycled anodes. These elements will be continued to be followed. However, the effects of these trace elements are not within the scope of this work. They will be subject of a future project.

4.4 Summary

The investigation on the production units and the first series of experiments have helped greatly focus the work. Some solutions have been suggested to the plant to improve their operation and manufacturing process.

1. Determining the trace elements (Fe, Ca, Si, Na) is a key control variable and their content should be used as an indication of the contamination during the entire manufacture process.

2. Control of the impurities mixed in the production process:

a) The inner lining of the calcinations kilns should be replaced regularly because the lining material can increase the Ca and Si of calcined coke (see Figure 4.20).

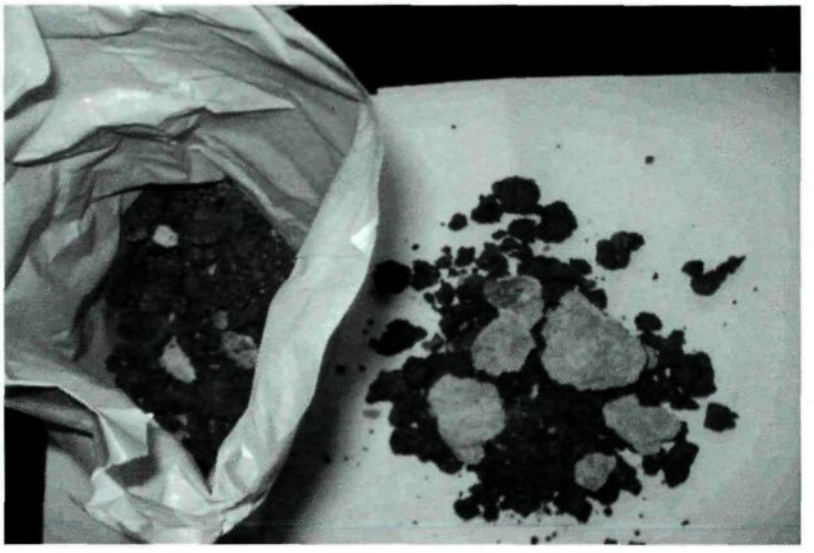

Figure 4.20 The lining material mixed with calcined coke

b) The cooling section of the coke calcination kiln should be fixed regularly because there is no lining inside the kiln; and the inner wall of the this part can easily get rusty and peel leading to increased Fe in calcined coke (see Figure 4.21).

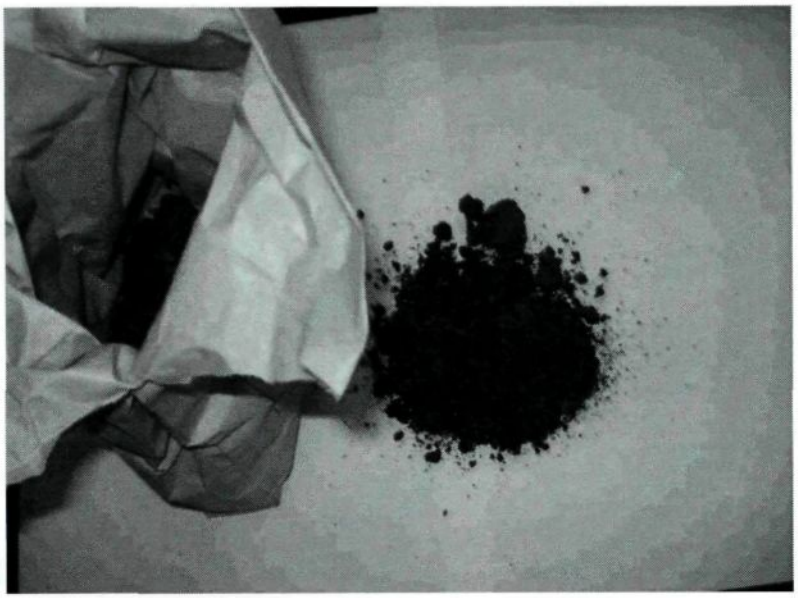

Figure 4.21 The rust mixed with the calcined coke

c) The electromagnetic iron-separator above the transportation belts should be cleaned frequently because of the many captured iron wires coming from the raw materials and other parts of the production (see Figures 4.22 and 4.23).

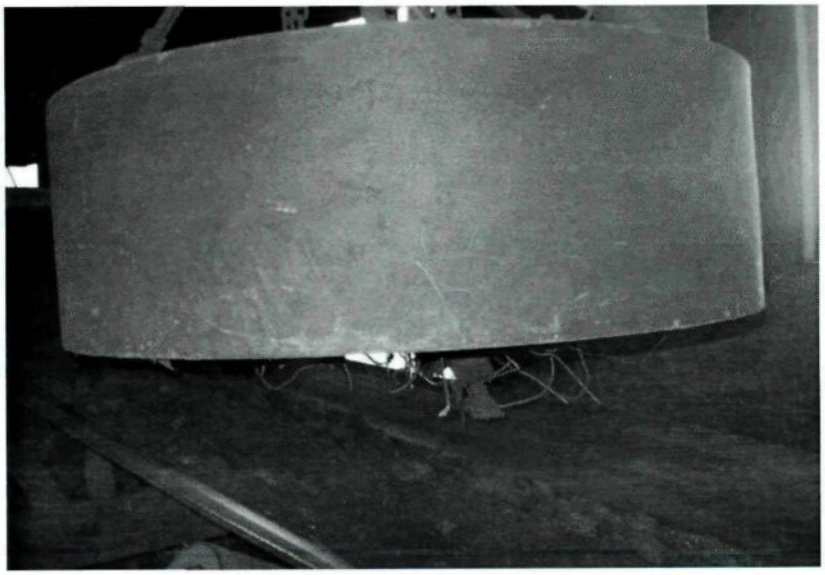

Figure 4.22 The iron-separator with lots of iron wires (before clean-up)

Figure 4.23 The iron-separator (after clean-up)

3. Rare earth elements serve as catalysts in secondary cracking process of refining heavy oil. Thus the rare earth elements La and Ce are the residual impurities of petroleum coke. It was observed that the La and Ce coming from coke as well as from butts can accumulate in anodes during the anode manufacture process. The baked anode might contain higher La and Ce content than the raw material and recycled butts. The presence of La and Ce increases CO_2 and air reactivities of anodes leading to increased anode consumption.

Chapter 5

Correlation between anode formulation and anode properties

5.1 Introduction

In Chapter 4, the characterization and analysis of raw material have been discussed. The properties of the currently used anodes were determined in order to correlate the current anode recipe and anode properties. As shown in Chapter 4, Figure 4.19 shows the type of coke structure found in the anode paste. This is likely to increase the porosity and air permeability of the anode. Thus, the quantity of small particle size fraction group with maximum particle size less than 12mm was adjusted in the paste formulation experiments to increase the contact area of coke and pitch and to decrease the effect of coke porosity. The correlation between anode formulation and anode properties is discussed in this chapter.

5.2 Results

5.2.1 The results of small particle size recipes

Tables 5.1 to 5.8 present the recipes (coke particle size distribution), pitch type, and kneading conditions used in anode formulation. As shown in these tables, the same pitch in same quantity (15% wt) and the same kneading conditions were always used. Only the percentage of coarse and fine particle fraction groups were changed. The formulation No 1 was taken as the reference recipe (Table 5.1). In the recipe 2, the percentage of coarse

fraction was increased (10-6mm) and that of the fine fraction was decreased (< 3mm). In 3rd and 4th recipes, the largest diameter size was eliminated. 8-6 mm fraction was used instead of 10-6mm fraction. In the 3rd recipe, the same percentages as the 1st recipe were used. The only difference was the particle size range of the coarse fraction. In the 4th recipe, this fraction was increased wheres the fines were slightly decreased. From 5th to 8th recipe, the coarse fraction was completely eliminated. The percent of 6-3 mm fraction was taken as the total of 10-6 mm and 6-3 mm fractions for recipe No.7. For the others, this fraction was either increased (recipe No.5) or decreased (recipe No.6 and 8). The balance is corrected by adjusting the fine content.

Table 5.1 The formulation conditions for No.1 small size recipe

No.1 small size recipe	Particle Size(mm)	Percentage (%)
Coke coarse	10 ~ 6	9.8
Coke inter-medium	6 ~ 3	6.9
Coke fine	< 3	35.1
Dust	BM	28.2
Recycled coarse	10 ~ 3	8
Recycled fine	< 3	12
Pitch	-	15
Kneading Temperature (°C)		Kneading Time (min)
Range	Actual	
160±5	165	10

Table 5.2 The formulation conditions for No.2 small size recipe

No.2 small size recipe	Particle Size (mm)	Percentage (%)
Coke coarse	10 ~ 6	15.8
Coke inter-medium	6 ~ 3	6.9
Coke fine	< 3	29.1
Dust	BM	28.2
Recycled coarse	10 ~ 3	8
Recycled fine	< 3	12
Pitch	-	15
Kneading Temperature (°C)		Kneading Time (min)
Range	Actual	
160±5	165	10

Table 5.3 The formulation conditions for No.3 small size recipe

No.3 small size recipe	Particle Size (mm)	Percentage (%)
Coke coarse	8 ~ 6	9.8
Coke inter-medium	6 ~ 3	6.9
Coke fine	< 3	35.1
Dust	BM	28.2
Recycled coarse	8 ~ 3	8
Recycled fine	< 3	12
Pitch	-	15
Kneading Temperature (°C)		Kneading Time (min)
Range	Actual	
160±5	165	10

Table 5.4 The formulation conditions for No.4 small size recipe

No.4 small size recipe	Particle Size (mm)	Percentage (%)
Coke coarse	8 ~ 6	15.8
Coke inter-medium	6 ~ 3	6.9
Coke fine	< 3	29.1
Dust	BM	28.2
Recycled coarse	8 ~ 3	8
Recycled fine	< 3	12
Pitch	-	15
Kneading Temperature (°C)		Kneading Time (min)
Range	Actual	
160±5	165	10

5.5 The formulation conditions for No.5 small particle size recipe

No.5 small size recipe	Particle Size (mm)	Percentage (%)
Coke inter-medium	6 ~ 3	22.7
Coke fine	< 3	29.1
Dust	BM	28.2
Recycled coarse	8 ~ 3	8
Recycled fine	< 3	12
Pitch	-	15
Kneading Temperature (°C)		Kneading Time (min)
Range	Actual	
160±5	165	10

Table 5.6 The formulation conditions for No.6 small particle size recipe

No.6 small size recipe	Particle Size (mm)	Percentage (%)
Coke inter-medium	6 ~ 3	15.8
Coke fine	< 3	36
Dust	BM	28.2
Recycled coarse	8 ~ 3	8
Recycled fine	< 3	12
Pitch	-	15
Kneading Temperature (°C)		Kneading Time (min)
Range	Actual	
160±5	165	10

Table 5.7 The formulation conditions for No.7 small particle size recipe

No.7 small size recipe	Particle Size (mm)	Percentage (%)
Coke inter-medium	6 ~ 3	16.7
Coke fine	< 3	35.1
Dust	BM	28.2
Recycled coarse	8 ~ 3	8
Recycled fine	< 3	12
Pitch	pitch	15
Kneading Temperature (°C)		Kneading Time (min)
Range	Actual	
160±5	165	10

Table 5.8 The formulation conditions for No.8 small particle size recipe

No.8 small size recipe	Particle Size (mm)	Percentage (%)
Coke inter-medium	6 ~ 3	9.8
Coke fine	< 3	42
Dust	BM	28.2
Recycled coarse	8 ~ 3	8
Recycled fine	< 3	12
Pitch	-	15
Kneading Temperature (°C)		Kneading Time (min)
Range	Actual	
160±5	165	10

Table 5.9 presents the measured properties of the anodes prepared using the above recipes. From this table, it can be clearly seen that No.4 recipe in which the maximum particle size was 8 mm had better properties than the anodes made with the other recipes. The air reactivity residue was higher than those of all the others with the exception of recipe 5. The recipe 5 anodes had slightly higher residue for air reactivity; however, its CO_2 reactivity residue was much lower compared to that of the No.4 recipe anode showing higher CO_2 reactivity. Also, No.4 recipe anode had the lowest permeability among others. Thus, the No.4 recipe was chosen to improve the properties further by optimizing the recycled butt content.

Table 5.9 The properties of eight anodes prepared with different small particle size recipes

Test No.	Air reactivity (%)	CO_2 reactivity (%)	Air permeability (npm)	Maximum particle size (mm)
1	56.07	81.22	11.06	10
2	56.05	80.39	7.21	10
3	55.95	83.51	4.67	8
4	60.30	85.44	4.06	8
5	61.95	76.52	4.81	6
6	53.42	78.81	9.04	6
7	56.43	80.42	9.46	6
8	55.54	83.38	11.67	6

Tables 5.10 to 5.13 show the modification of butt content (recycled coarse and recycled fine) in small particle recipe No.4, and Table 5.14 presents the properties of the anodes prepared with these recipes. The results of recycled butt tests showed that the properties of the No.11 recipe with 12% coarse recycled butt and 8% fine recycled butt were better than the rest of the small particle size recipes since it had the highest residue for CO_2 and air reactivity tests and the lowest permeability of among the other recipes of butt percentage adjustment (recipes 9, 10, and 12). Next, the anodes coke particle sizes were

prepared and their properties were compared with those of the anode of No.11 recipe. This was carried out to verify the validity of the small particle recipe as the best one.

Table 5.10 The recycled butt test 1 of No.4 small size recipe (Recipe 9)

No.9 small size recipe	Particle Size(mm)	Percentage (%)
Coke coarse	8 ~ 6	15.8
Coke inter-medium	6 ~ 3	6.9
Coke fine	< 3	29.1
Dust	BM	28.2
Recycled coarse	8 ~ 3	6
Recycled fine	< 3	14
Pitch	pitch	15
Kneading Temperature (°C)		Kneading Time (min)
Range	Actual	
160±5	165	10

Table 5.11 The recycled butt test 2 of No.4 small size recipe (Recipe 10)

No.10 small size recipe	Particle Size(mm)	Percentage (%)
Coke coarse	8 ~ 6	15.8
Coke inter-medium	6 ~ 3	6.9
Coke fine	< 3	29.1
Dust	BM	28.2
Recycled coarse	8 ~ 3	8
Recycled fine	< 3	12
Pitch	pitch	15
Kneading Temperature (°C)		Kneading Time (min)
Range	Actual	
160±5	165	10

Table 5.12 The recycled butt test 3 of No.4 small size recipe (Recipe 11)

No.11 small size recipe	Particle Size(mm)	Percentage (%)
Coke coarse	8 ~ 6	15.8
Coke inter-medium	6 ~ 3	6.9
Coke fine	< 3	29.1
Dust	BM	28.2
Recycled coarse	8 ~ 3	12
Recycled fine	< 3	8
Pitch	pitch	15
Kneading Temperature (°C)		Kneading Time (min)
Range	Actual	
160±5	165	10

Table 5.13 The recycled butt test 4 of No.4 small size recipe (Recipe 12)

No.12 small size recipe	Particle Size(mm)	Percentage (%)
Coke coarse	8 ~ 6	15.8
Coke inter-medium	6 ~ 3	6.9
Coke fine	< 3	29.1
Dust	BM	28.2
Recycled coarse	8 ~ 3	14
Recycled fine	< 3	6
Pitch	pitch	15
Kneading Temperature (°C)		Kneading Time (min)
Range	Actual	
160±5	165	10

Table 5.14 The properties of anodes prepared with modified recycled butt content

Test No.	Air reactivity (%)	CO_2 reactivity (%)	Air permeability (npm)	Coarse: fine (% Recycled butt)
9	59.05	85.36	4.33	6%:14%
10	59.83	84.22	4.18	8%:12%
11	62.76	89.24	2.79	12%:8%
12	61.95	86.50	3.56	14%:6%

5.2.2 The results of big particle size recipes

Tables 5.15 to 5.17 present the recipes for big particle size formulation. In these recipes, the coarse fraction range was 15-9 mm compared to 8-6 mm of the small particle recipe. The quantity and type of pitch and kneading conditions were the same as the small particle recipes. The anode properties are presented in Table 5.18. The results showed that the properties of big particle recipes were worse than those of the small particle recipes, especially the recipe No 11 which was the best among others. The results proved that the use of the small particle recipe led to better quality anodes probably by improving the wetting of coke by pitch, thus, the penetration behavior of pitch.

Table 5.15 The formulation conditions for No.1 big particle recipe

No.1 big size recipe	Particle Size(mm)	Percentage (%)
Coke coarse	15 ~ 9	9.8
Coke inter-medium	9 ~ 3	6.9
Coke fine	< 3	35.1
Dust	BM	28.2
Recycled coarse	15 ~ 3	8
Recycled fine	< 3	12
Pitch	pitch	15
Kneading Temperature (°C)		Kneading Time (min)
Range	Actual	
160±5	165	10

Table 5.16 The formulation conditions for No.2 big particle recipe

No.2 big size recipe	Particle Size(mm)	Percentage (%)
Coke coarse	15 ~ 9	15.8
Coke inter-medium	9 ~ 3	6.9
Coke fine	< 3	29.1
Dust	BM	28.2
Recycled coarse	15 ~ 3	8
Recycled fine	< 3	12
Pitch	pitch	15
Kneading Temperature (°C)		Kneading Time (min)
Range	Actual	
160±5	165	10

Table 5.17 The formulation conditions for No.3 big particle recipe (base recipe)

No.3 big size recipe	Particle Size(mm)	Percentage (%)
Coke coarse	12 ~ 6	11.3
Coke inter-medium	6 ~ 3	9.4
Coke fine	< 3	30.4
Dust	BM	28.3
Recycled coarse	12 ~ 3	8
Recycled fine	< 3	12
Pitch	pitch	15
Kneading Temperature(°C)		Kneading Time (min)
Range	Actual	
160±5	165	10

Table 5.18 The properties of anodes prepared with big particle recipes

Test No.	Air reactivity (%)	CO_2 reactivity (%)	Air permeability (npm)	Maximum particle size (mm)
1	56.07	81.22	17.06	15
2	57.80	79.30	19.50	15
3	59.83	80.90	10.79	12

5.3 Results of the tests on the actual production line and discussion

After testing a large number of recipe variations in the laboratory, further testing was undertaken on the actual production line by separating the anode formulation experiments into three groups. The properties presented below are the average values for a number of anodes produced on the actual production line (details are not given due to confidentiality). The three groups are:

1) The small particle group

2) The big particle group

3) Base recipe (see Table 5.17). This is the recipe which was used in the actual anode manufacturing process before this study.

Table 5.19 shows the comparison of the properties of anode samples tested for different groups.

Table 5.19 Comparison of properties for different groups

Recipe	CO_2 reactivity 960°C (%) residue	Air reactivity 525°C (%) residue	Air permeability (npm)
Small group	89.44	60.21	2.58
Big group	83.55	61.85	8.85
Base recipe	79.71	58.51	7.32

The recipe of small particle size group (Recipe No.11) that was tested on the pilot line shows the best results in the industry. It has been used on the actual anode paste operation since then. This recipe was also selected to do the TGA tests which will be presented in the next chapter. Comparing the results of small particle recipe tests and big particle recipe tests, the correlation between the maximum particle size and the anode properties were illustrated in the following figures.

Figures 5.1 and 5.2 show how the anode reactivity and permeability change with maximum coke particle size. The results indicate that the 8 mm recipe resulted in better anode properties compared to the rest of the recipes, especially Figure 5.2 shows that the air permeability value at 8 mm is better than others. That means the 8 mm is an optimum point of the recipe formulation. If the maximum particle is less than 8 mm, the pitch content may need to be increased due to increased surface area; otherwise, the wetting and penetration behavior of the binder-matrix (mixture of dust and pitch) may be affected adversely. On the other hand, if the maximum particle size is bigger than 10 mm, there are large quantities of pores and fissures inside the coke, this situation can increase the air permeability. Even though the 8 mm recipe does not have the lowest air reactivity (which corresponds to the highest residual percentage in the figure), the variation in air reactivity values is not significant, especially when this is compared to the gain in terms of CO_2 reactivity. The CO_2 reactivity is the best (the residual percentage is the highest) for the 8 mm recipe.

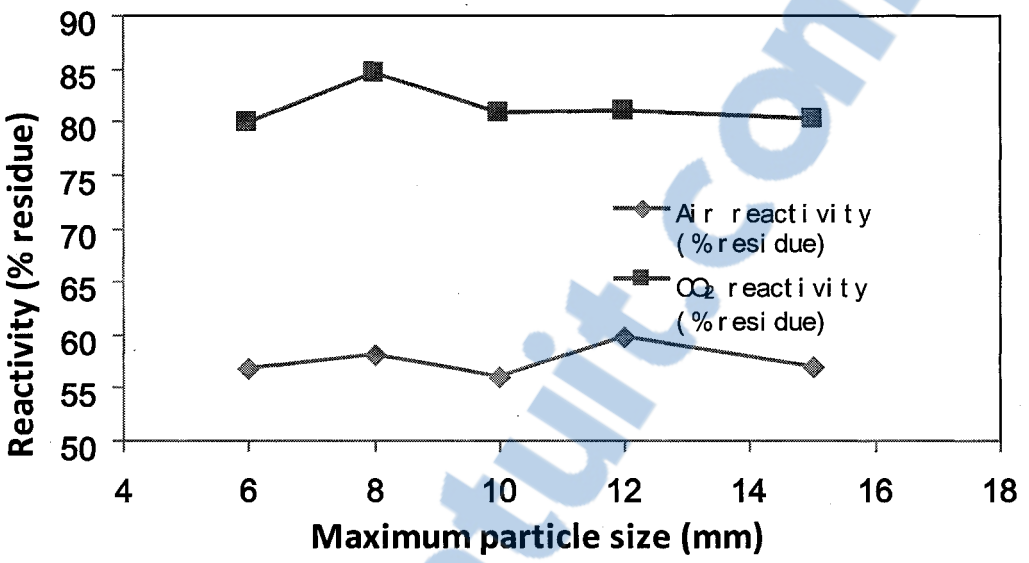

Figure 5.1 The correlation between anode reactivities and maximum particle size

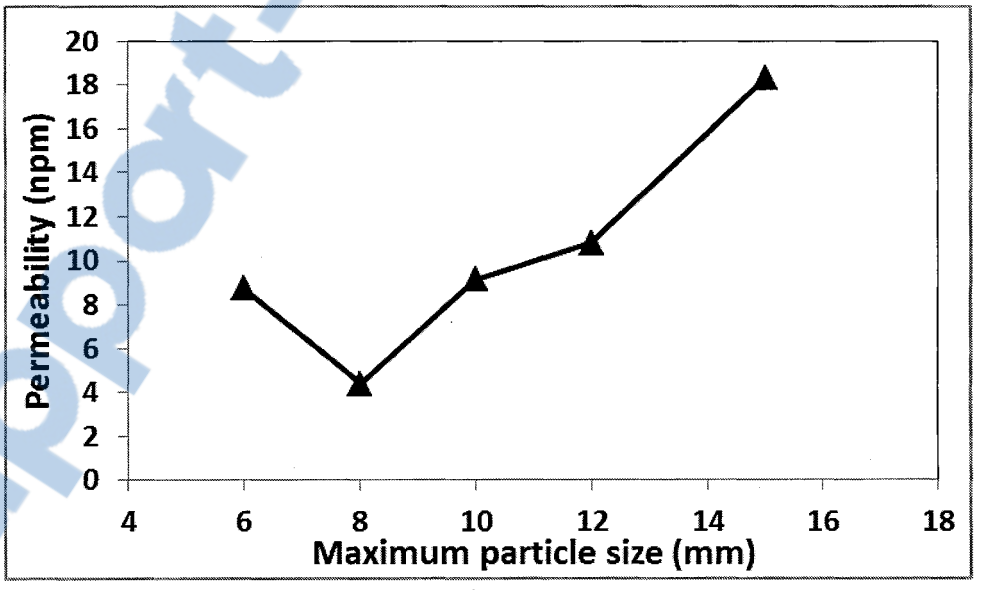

Figure 5.2 The correlation between anode air permeability and maximum particle size

5.4 Summary

The No.11 recipe was found to perform better than other size recipes. Because the plant requested 15% of pitch content, the 8 mm maximum particle size was optimum for this level of pitch. Thus, at optimum conditions, the pitch/fines binder matrix penetrates the fissures and pores of the coarse petroleum coke particle and thinly coats the particles.

Chapter 6

Thermogravimetric experiments and analysis of devolatilisation kinetics

6.1 Introduction

In the last two chapters, the determination of an anode recipe leading to best anode properties was summarized. Afterwards, the anodes prepared with the best anode recipe (recipe no. 11) were baked under different conditions and their properties were measured. These properties were correlated with the baking conditions. The aim was to identify the baking conditions which will improve the anode properties further. Also, the volatiles released (tar, H_2, and CH_4) were analyzed and their devolatilisation kinetics were determined. The results are presented in this chapter.

Baking experiments with the TGA facilitate the determination of the effect of baking conditions on anode properties. The kinetic expressions obtained from the TGA analysis make the determination of quantity, time, and temperature of volatile release in the furnace possible. Utilisation of this information wisely can lead to not only the improvement of the quality but also increase in the combustion efficiency of condensable (tar) and non-condensable gases (H_2 and CH_4) to reduce the energy consumption.

6.2 Results

6.2.1 Thermogravimetric experiments

The TGA and volatiles tests were carried out in the CURAL laboratory of the University of Quebec at Chicoutimi. The TGA results are presented in Figures 6.1 and 6.2. Table 6.1 presents the baking conditions and the measured anode properties for the five anodes prepared using recipe 11 as well as those of the anode prepared using the base recipe.

Figure 6.1 shows the weight loss curves of the anode samples. Anodes 1 to 4 are baked at the same heating rate. The soaking times can't be seen on this figure since the weight loss is plotted as a function of temperature, and there is a direct relationship between temperature and time through the heating rate until the final baking temperature is reached after which the soaking period starts. Therefore, the weight loss curves of anodes 1 and 3 should be the same since their final baking temperatures are the same. This is the case as it can be seen from the figure. Slight differences can be attributed to the non-homogeneity of the anodes. The baking temperature of anode 2 was lower whereas that of anode 4 was higher than the other experiments. Anode 5 was baked using a lower heating rate. The weight loss for this anode is higher at a given temperature compared to those of the other anodes. When the anode is heated slowly, the contact time (baking time) between the anode and the gas is longer, consequently, it loses more weight compared to the anodes which are baked more rapidly.

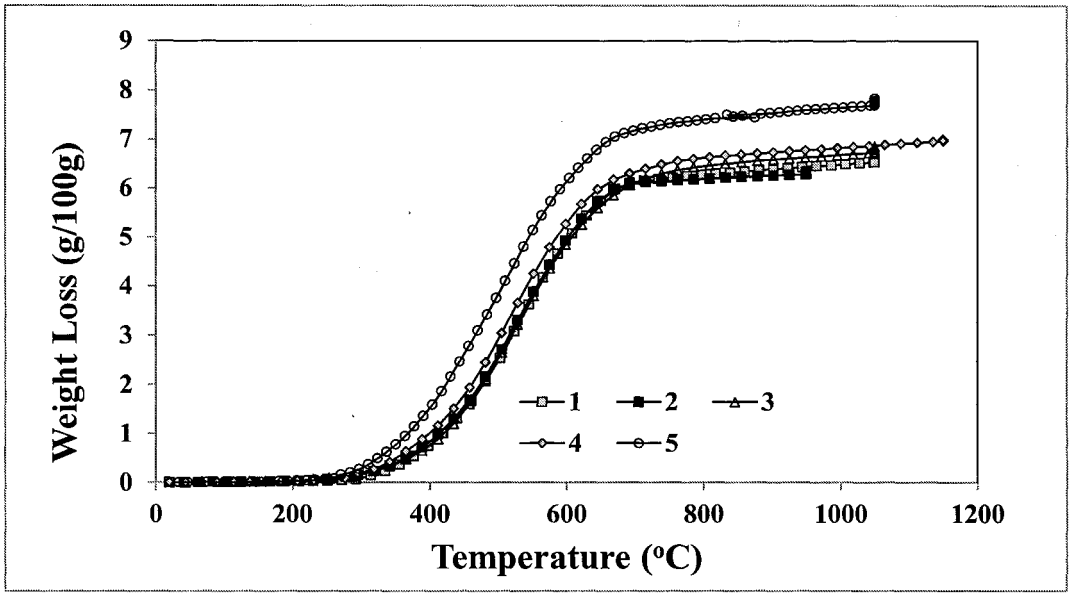

Figure 6.1 Weight loss vs. temperature data of the anode samples

The weight loss vs. time data is presented in Figure 6.2. In this figure, the soaking times can be seen. Weight loss for the experiment performed at a lower heating rate (anode 5) is less than the weight loss of others at a given time. The reason is that it takes longer to reach the same temperature, and at any given time the temperature of this anode is lower compared to the temperatures of other anodes. Anode 1 is heated to 1050°C followed by 8 hours of soaking. Anodes 1, 2, and 4 have the same soaking times. Anode 4 was heated to a higher temperature (1150°C) which means it was heated for a longer time to reach this temperature. When anodes 1 to 4 are compared, it can be seen that anode 4 lost more weight. Soaking time for this anode was also 8h. The reverse is true for anode 2 which has the lowest final temperature (950°C). Anode 3 has higher soaking time (12 h) compared to other anodes. These can clearly be observed from the figure.

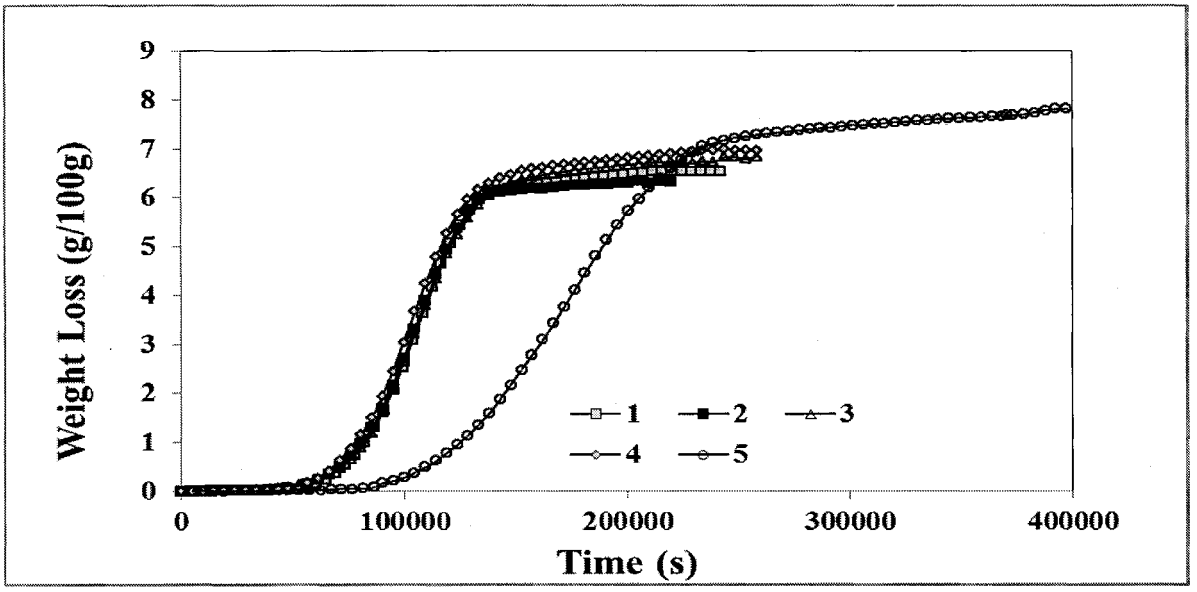

Figure 6.2 Weight loss vs. time data of the anode samples

The carbon dioxide and air reactivities as well as the air permeabilities of baked anodes were measured and the results are presented in Tables 6.1. The reactivities are given as the % residue remained after the reactivity tests. Therefore, higher the residue, lower the reactivity. Decreasing the maximum baking temperature and consequently the baking time increased the reactivity (decreased the residue of both CO_2 and air reactivity tests) and increased the air permeability of the anodes. This shows that the anode properties deteriorated. Increasing the soaking time had the reverse effect. Increasing maximum baking temperature and time also improved the anode properties as expected. Increasing the baking time by decreasing the heating rate improved the reactivity, however, worsened the permeability of anodes. It can be seen from this table that the baking conditions influence the CO_2 reactivity more than the air reactivity. Permeability was affected most by the baking temperature.

Table 6.1 The results of TGA tests

	Anode properties			Anode baking conditions			
Anode	**CO_2 reactivity (%)**	**Air reactivity (%)**	**Air permeability (npm)**	**Maximum temperature (°C)**	**Soaking time (h)**	**Baking time (h)**	**Heating rate (°C/h)**
Base recipe	79.7	58.5	7.3	1050	8	68	17.5
1	89.4	60.2	2.9	1050	8	68	17.5
2	80.3	58.1	7.5	950	8	61	17.5
3	91.3	62.6	2.7	1050	12	71	17.5
4	95.7	65	2.1	1150	8	73	17.5
5	93.5	63.2	2.5	1050	8	113	10

First line in Table 6.1 gives the properties and the baking conditions for an anode sample produced using a base recipe. Anode samples except anode 2 have better properties than those of the one made with base recipe. Anodes 3 and 5 are baked with higher baking times compared to those of others. Their properties are better than those of anode 1. Anode 4 which was heated for a longer period and to a higher temperature is better than others. Anode 2 has the worst properties because it was heated in a shorter time and the baking temperature was lower than those used in the other recipes. Thus, the TGA results show that the baking time and the maximum temperature are both important for anode properties. However, for industry, longer baking time and higher temperature mean more energy consumption; and this would raise the production costs. In the next part, volatile analysis results indicate how to make use of volatiles to save energy. Anode sample made with base

recipe was used to test the TGA system, and the volatile analysis was not done for this test; however, the rest of the anode samples from 1 to 5 were tested for the volatiles content.

6.2.2 Volatiles analysis

If the fuel and the volatiles (tar, H_2 and CH_4) are burnt efficiently in the anode baking furnace, the energy efficiency can be improved. Therefore, the information on the release of these volatiles (quantity, time, temperature range) is very crucial for the baking furnace performance. This information also can be used as an input in the baking furnace models. Since their behaviour depends on the raw materials used, they have to be measured specifically for a given anode.

The instantaneous and the cumulative amounts of H_2, CH_4, and tar at different temperatures for all the baking conditions were calculated following the procedure described in section 3.3.1 and 3.3.2 and are summarized in Table 6.2.Figures 6.3, 6.5, 6.7, 6.9, and 6.11 show the instantaneous amount of H_2, CH_4, and tar released while Figures 6.4, 6.6, 6.8, 6.10, and 6.12 show their cumulative amounts at different temperatures for anodes 1 to 5, respectively.

Figure 6.3 shows that there was small amount of tar coming out up to 250°C. After that, there was a marked increase in tar content coming out of the anode sample. The amount of tar was maximum at a temperature of about 500°C. After that, there was a decrease in tar content and the amount of tar was negligible after a temperature of 700°C. Thus, during the baking of green anodes, one must take special care for tar in the

temperature range of about 350°C to 650°C. H_2 was found to start evolving at around 400°C and reached a maximum at around 550°C. The rate of production of H_2 was nearly constant up to the temperature of about 700°C. After 700°C, there was a marked drop in H_2 production. Thus, the energy from H_2 can be utilized for baking of the green anodes at a temperature range of 550°C to 700°C. Any additional energy used during this temperature range will make it possible to reduce the use of external energy for baking. CH_4 released nearly at 300°C and reached a maximum at around 450°C. The rate of production of CH_4 became constant at around 500°C After 550°C, the amount of CH_4 gradually reduced. After 700°C, there was a sharp drop in the CH_4 production. Thus, the energy from CH_4 can be utilized for baking of the green anodes at a temperature range of 500°C to 700°C.

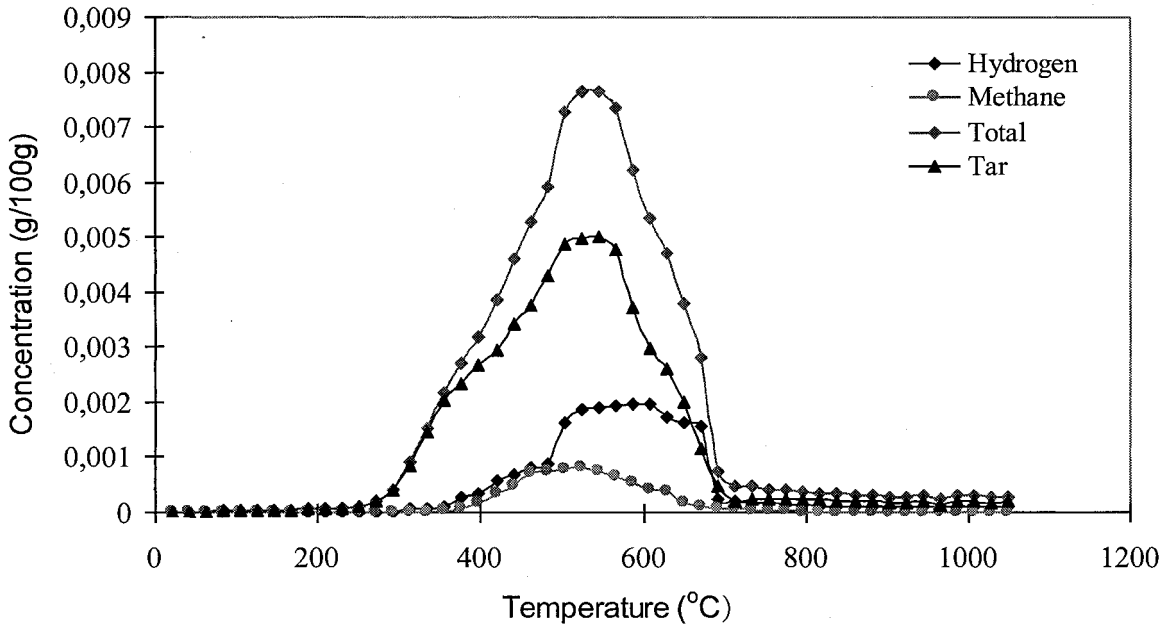

Figure 6.3 Comparison of instantaneous concentration of hydrogen, methane, tar and total volatiles for anode 1

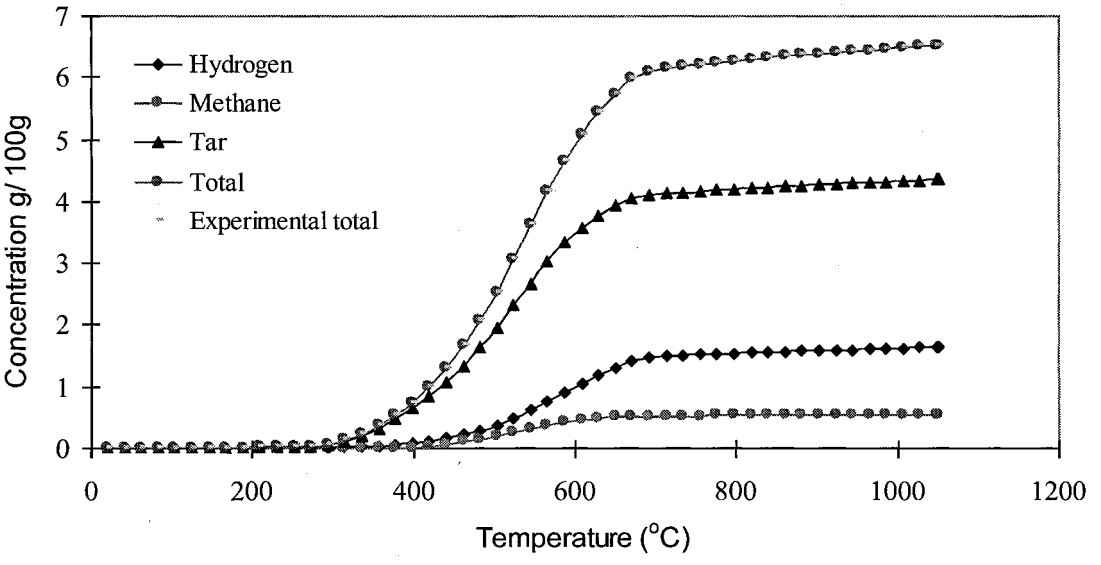

Figure 6.4 Comparison of calculated cumulative concentration of hydrogen, methane, tar and total volatiles and experimental total volatiles for anode 1

Figure 6.5 shows that the tar came out after 200°C. As the temperature increased, the amount of tar increased. At about 500°C, the amount of tar was maximum. After that, there was a decrease in tar content and the amount of tar was negligible after a temperature of 700°C. Thus, during the baking of green anodes, the temperature range of about 200°C to 700°C is critical for tar. H_2 release started at around 300°C and became constant at around 500°C. After 600°C, there was a big drop in H_2 production. Thus, the energy from H_2 can be utilized for baking of green anodes at a temperature range of 500°C to 700°C. During this temperature range, additional energy from H_2 combustion will help reduce the use of external energy for baking. CH_4 release started nearly at 300°C and reached a maximum at around 400°C. The rate of production of CH_4 became constant up to 650°C. After 550°C,

the amount of CH_4 released gradually reduced. After 700°C, there was negligible CH_4 production. Thus, the energy from CH_4 can be utilized for baking of green anodes at a temperature range of 400°C to 650°C.

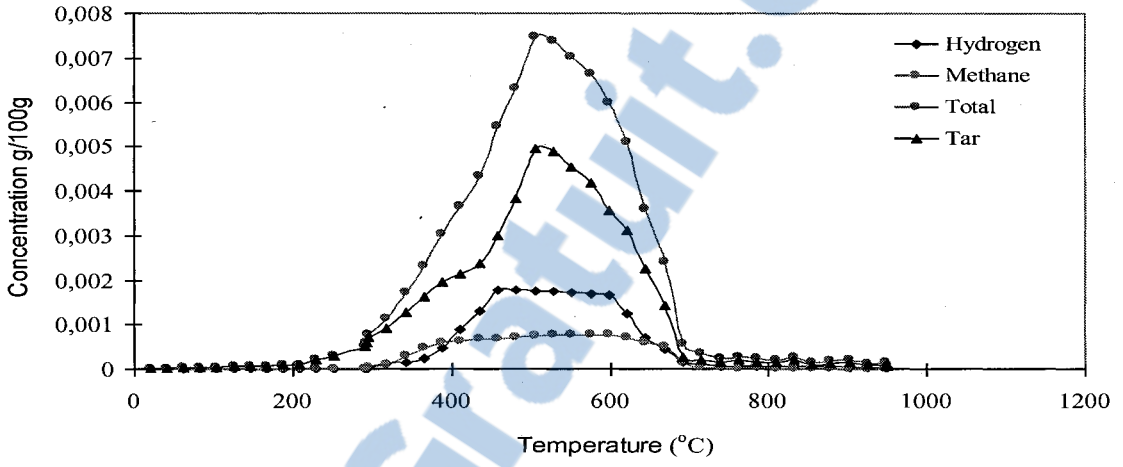

Figure 6.5 Comparison of instantaneous concentration of hydrogen, methane, tar and total volatiles for anode 2

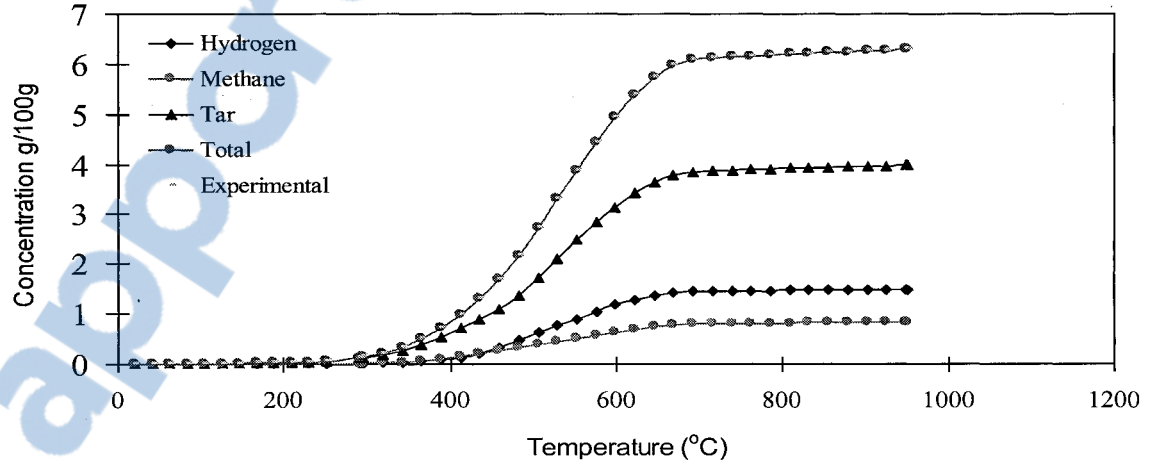

Figure 6.6 Comparison of calculated cumulative concentration of hydrogen, methane, tar and total volatiles and experimental total volatiles for anode 2

Figure 6.7 shows that there was little amount of tar coming out until a temperature of 200°C. After that, there was a marked increase in tar content coming out of the anode sample. The amount of tar was maximum at about 550°C. After that, there was a decrease in tar content and the amount of tar was negligible after a temperature of 800°C. Thus, during the baking of green anodes, one must take special care for tar in the temperature range of about 200°C to 800°C. H_2 was found to start evolving at around 350°C and reached a maximum at around 550°C. The rate of production of H_2 was nearly constant up to a temperature of about 700°C. After 700°C, there was a marked drop in H_2 production. Thus, the energy from H_2 can be utilized for baking of the green anodes at a temperature range of 550°C to 700°C. The additional energy use during this temperature range will make it possible to reduce the use of external energy for baking. CH_4 released nearly at 300°C and reached a maximum at around 450°C. The rate of production of CH_4 became constant at around 500°C. After 600°C, the amount of CH_4 gradually reduced. After 700°C, there was a clear drop in CH_4 production. Thus, the energy from CH_4 can be utilized for the baking of green anodes at a temperature range of 500°C to 700°C.

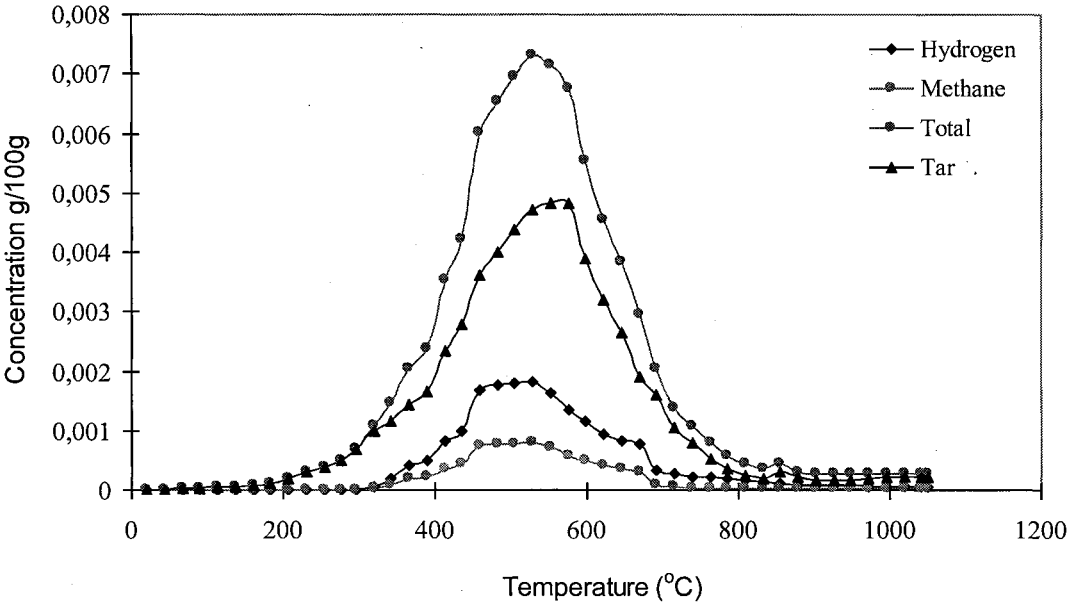

Figure 6.7 Comparison of instantaneous concentration of hydrogen, methane, tar and total volatiles for anode 3

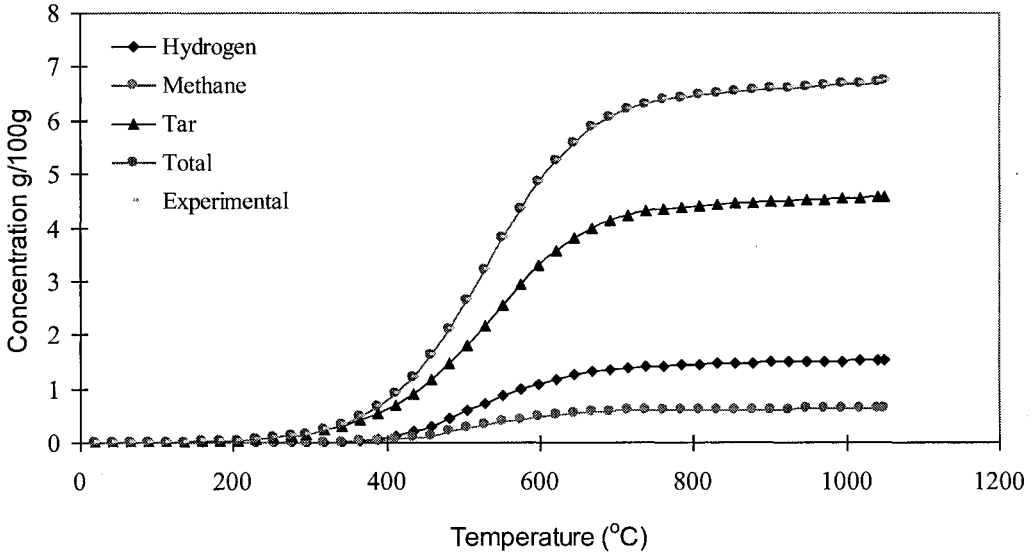

Figure 6.8 Comparison of calculated cumulative concentration of hydrogen, methane, tar and total volatiles and experimental total volatiles for anode 3

Figure 6.9 shows that the tar came out after 200°C. As the temperature increased, the amount of tar increased. At about 550°C, the amount of tar was maximum. After that, there was a decrease in tar evolution and the amount of tar was negligible after a temperature of 700°C. Thus, during the baking of green anodes in the temperature range of about 200°C to 700°C, special attention must be paid to tar. H_2 release started at around 300°C and reached maximum at around 500°C. After 650°C, there was a significant drop in H_2 production. Thus, the energy from H_2 can be utilized for the baking of green anodes within the temperature range of 450°C to 700°C. The additional energy use during this temperature range will make it possible to reduce the use of external energy for baking. CH_4 release started nearly at 300°C and there was a visible peak appearing in the temperature range of 400°C to 550°C; and, in the same range, the amount of CH_4 reached a maximum at around 500°C. After 550°C, the amount of CH_4 gradually reduced. After 700°C, there was negligible CH_4 production. Thus, the energy from CH_4 can be utilized for the baking of green anodes at a temperature range of 400°C to 600°C.

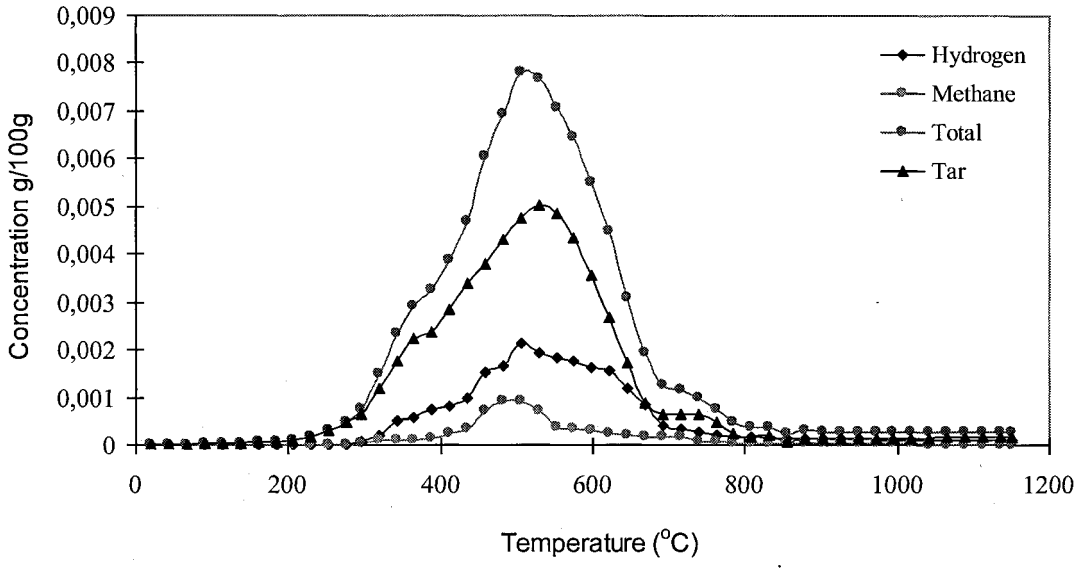

Figure 6.9 Comparison of instantaneous concentration of hydrogen, methane, tar and total volatiles for anode 4

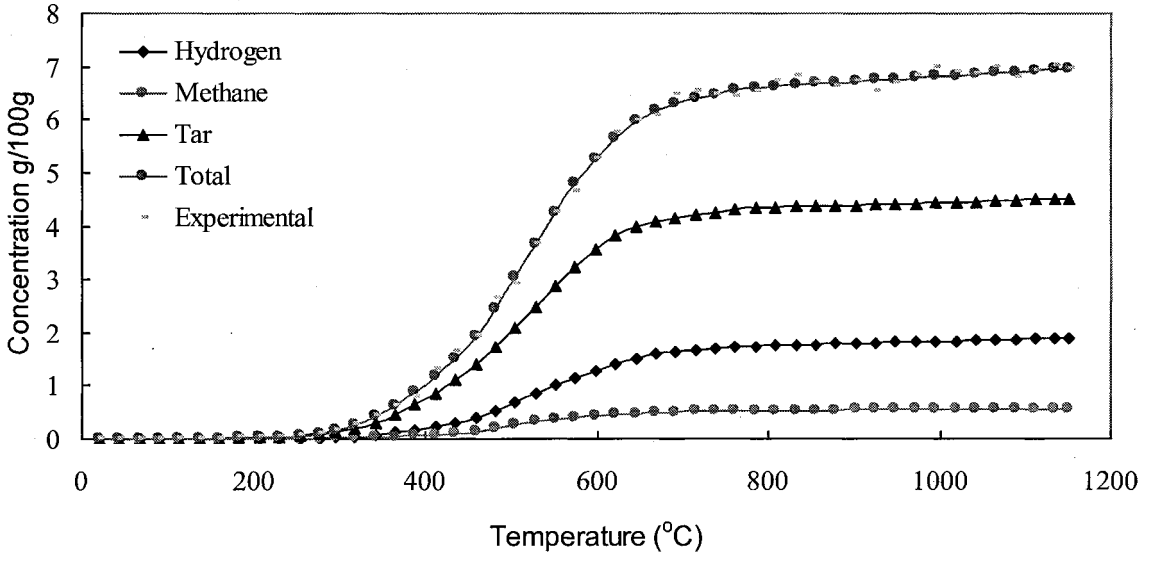

Figure 6.10 Comparison of calculated cumulative concentration of hydrogen, methane, tar and total volatiles and experimental total volatiles for anode 4

Figure 6.11 shows that before 200°C, there was little amount of tar coming out. After that, a marked peak in tar content appeared in the temperature range of 200°C to 750°C. The maximum amount of tar was reached at a temperature of about 500°C. H_2 started to evolve at around 250°C; and there were two constant rate zones for H_2 production when there was an appreciable rate of production. At first, the rate of production of H_2 was nearly constant between the range of 300°C to 500°C. After that, the rate of production increased suddenly and remained constant in the range of 550°C to 700°C After 700°C, there was a marked drop in H_2 production. Thus the energy from H_2 can be utilized for the baking of green anodes at a temperature range of 550°C to 700°C. Though there was a constant rate of formation of H_2 in the range of 300°C to 500°C, the amount was not high enough. Thus, during the temperature range for H_2 evolution, H_2 combustion will make it possible to reduce the use of external energy for baking. CH_4 is released nearly at 300°C and reached a maximum at around 400°C After 500°C, the amount of CH_4 gradually reduced. After 600°C, CH_4 production became negligible. Thus the energy from CH_4 can be utilized for the baking of green anodes at a temperature range of 300°C to 600°C.

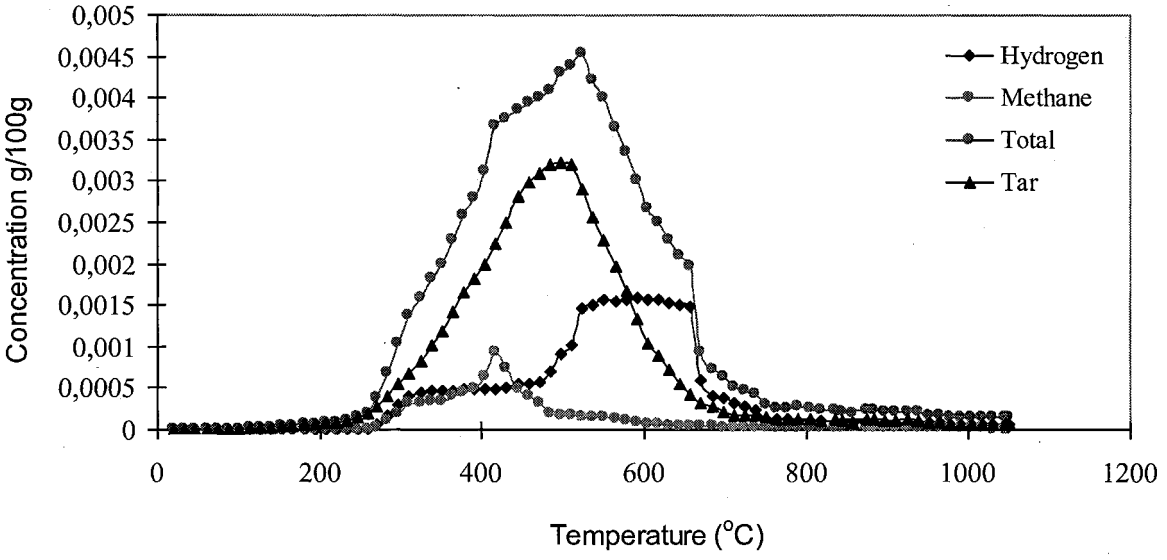

Figure 6.11 Comparison of instantaneous concentration of hydrogen, methane, tar and total volatiles for anode 5

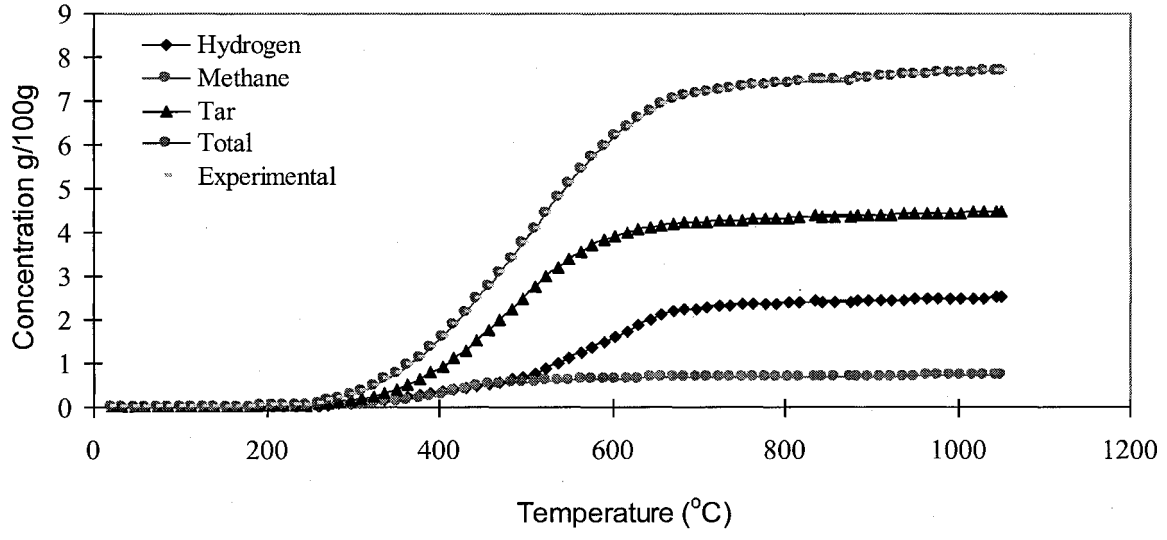

Figure 6.12 Comparison of calculated cumulative concentration of hydrogen, methane, tar and total volatiles and experimental total volatiles for anode 5

Figures 6.4, 6.6, 6.8, 6.10 and 6.12 show cumulative data for the anodes 1, 2, 3, 4, and 5, respectively. The total weight loss was calculated as the sum of the formation of tar, H_2, and CH_4. The total loss was found to be in agreement with the experimental weight loss. The observations were found to be similar for all the test conditions. It is also clear from the figures that the contribution in the total weight loss was the lowest for CH_4 and the highest for tar for all the cases. If the total amount of tar was compared for all the test conditions, it was observed that the amount of tar per 100 gm of anode was nearly the same (Table 6.2). The tendency of getting methane was more for anode 5 (Table 6.2). The amount of H_2 per 100 gm of anode was found to be markedly high also for anode 5 (Table 6.2). Thus, it was observed that amount of H_2 and CH_4 was more for low heating rate, but amount of tar remained nearly the same.

Figures 6.13, 6.14 and 6.15 compare the instantaneous hydrogen, methane, and tar concentrations, respectively, of all the baking tests.

Figure 6.13 shows the comparison of the amount of hydrogen formed at different temperatures for the five different baking tests. It is evident from the figure that the shape of graphs for anodes 1 to 4 is similar. However, for anode 5 for which a lower heating rate was used, the shape of the curve is somewhat different. H_2 started forming at a faster rate earlier compared to the other test conditions. It was also observed that there were two constant rate of formation zones for anode 5. Up to around 350°C, the amount of H_2 produced was maximum during this test, but as the temperature increased the amount released was decreased compared to those of the other anodes. The advantage was that a steady supply of H_2 can be obtained if the anodes are baked using the same conditions used

baking anode 5. Though theoretically it is expected that the graphs for the anodes 1 to 4 would be identical, yet some differences were observed. The differences in the results for anodes 1 to 4 are possibly due to non-homogeneity in the anode samples and difference in temperature and soaking times.

Figure 6.14 shows the comparison of the amount of methane formed at different temperatures for the 5 different baking tests. From the figure, it can be noted that the shape of graphs for anodes 1 to 4 was different from that of anode 5. The temperatures at which mathane release starts and maximum amount for CH_4 obtained were advanced due to lower heating rate. It could also be observed that the rate of formation of CH_4 for anode 5 suddenly dropped and decreased faster compared to the other anodes baked with different test conditions. Up to around 500°C, the rate of CH_4 production declined gradually. Compared to other test conditions, the amount of CH_4 was less in the same temperature range of 500°C to 700°C. The differences in the results for anodes 1 to 4 was again possibly due to non-homogeneity in the anode samples and differences in temperature and soaking times.

Figure 6.15 shows the comparison of the amount of tar formed at different temperatures for the 5 different baking conditions tests. From the figure, we could see that the peaks of graphs for all the test conditions are similar. However, in case of anode 5 where a lower heating rate was used, the area under the curve is smaller than those for the other anodes. Tar started forming and ended nearly at the same temperature range for all tests. The only difference that was observed is in the amount of tar production. It was also

observed that at around 550°C the amount of tar production for all the 5 test conditions reached maximum. Then, as the temperature was increased, there was a marked drop in tar formation for all 5 test conditions. Thus, the advantage of test condition used for anode 5 was that a smaller amount of tar had to be handled at the point of peak rate of formation.

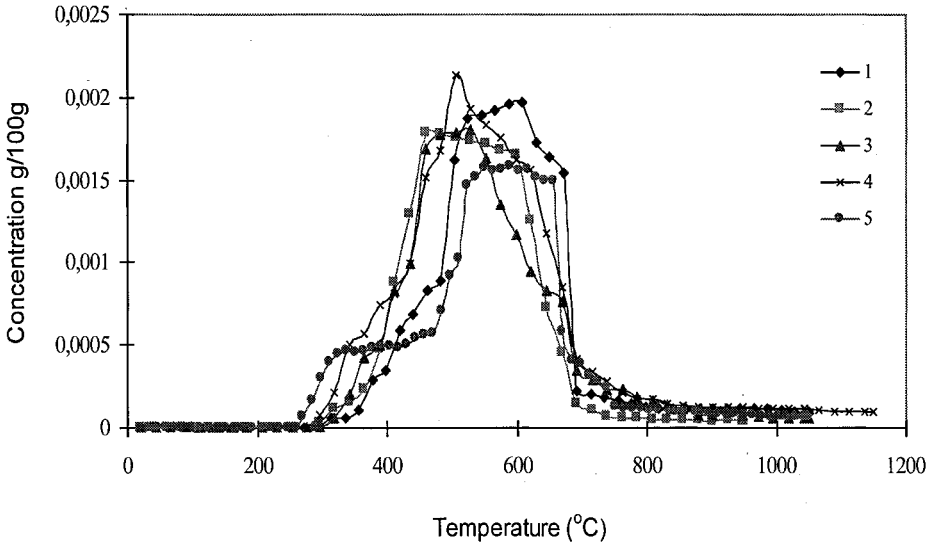

Figure 6.13 Comparison of instantaneous concentration of hydrogen for anode samples baked under five different conditions

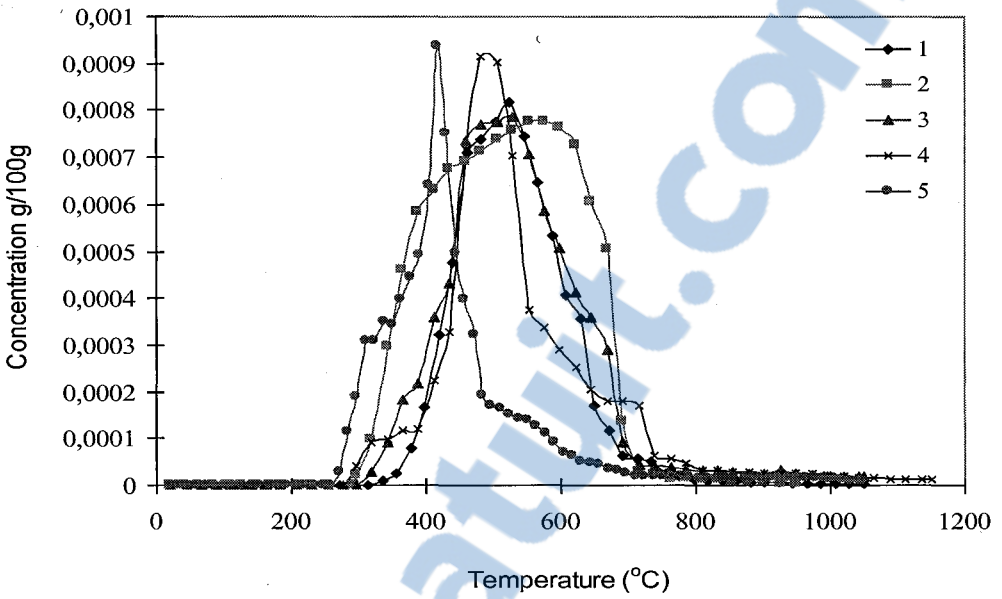

Figure 6.14 Comparison of instantaneous concentration of methane for anode samples baked under five different conditions

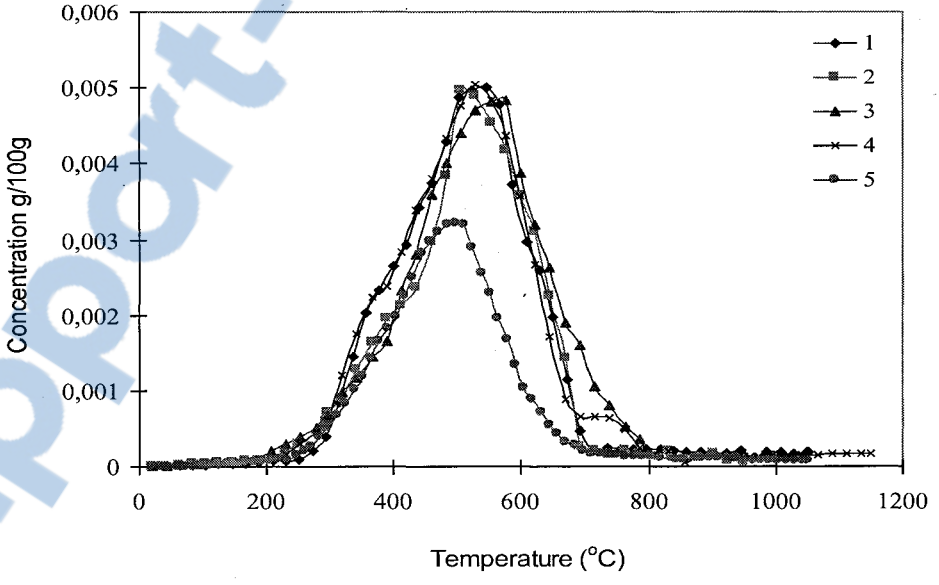

Figure 6.15 Comparison of instantaneous concentration of tar for anode samples baked under five different conditions

Table 6.2 gives the total amount of volatile components released under different baking conditions. This table shows that there is slight increase in H_2 release when the heating rate is lower.

As it can be seen from the data, the volatile release becomes negligible after 700°C for the anodes investigated during this study. Therefore, kinetic analysis was carried out only for the non-isothermal part (during heating) of the curve. It excludes the isothermal (soaking period) region. Although this analysis is empirical in nature, the rate expressions obtained can predict the emission of volatile gas components released during baking. Figures 6.16 and 6.17 give an example of kinetic parameter calculations.

Table 6.3 summarises the kinetic parameters for H_2, CH_4, and tar for all five test conditions. As it was indicated previously, the differences between the baking conditions for anodes 1 to 4 are the maximum temperatures and the soaking times. Therefore, the kinetic parameters of the non-isothermal regions should be the same. This can also be seen from the table. An average is calculated for each component for the tests carried out with anodes 1 to 4. As it can be seen from this table, the values of activation energy and pre-exponential constant decrease and the reaction order increases for H_2, and CH_4; however, those of the condensable gas increase when heating rate is decreased. It must be noted that the parameters are empirical. Although they are useful to calculate the amount of volatiles released for a particular coke, it is difficult to draw conclusions on their release mechanisms.

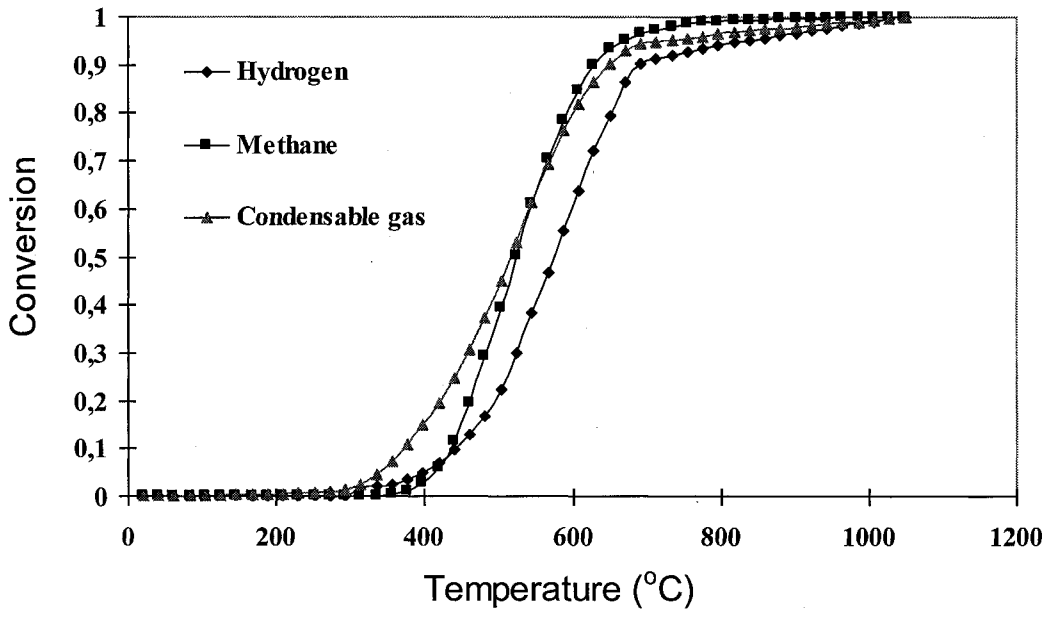

Figure 6.16 Conversions for hydrogen, methane and condensables for anode 1

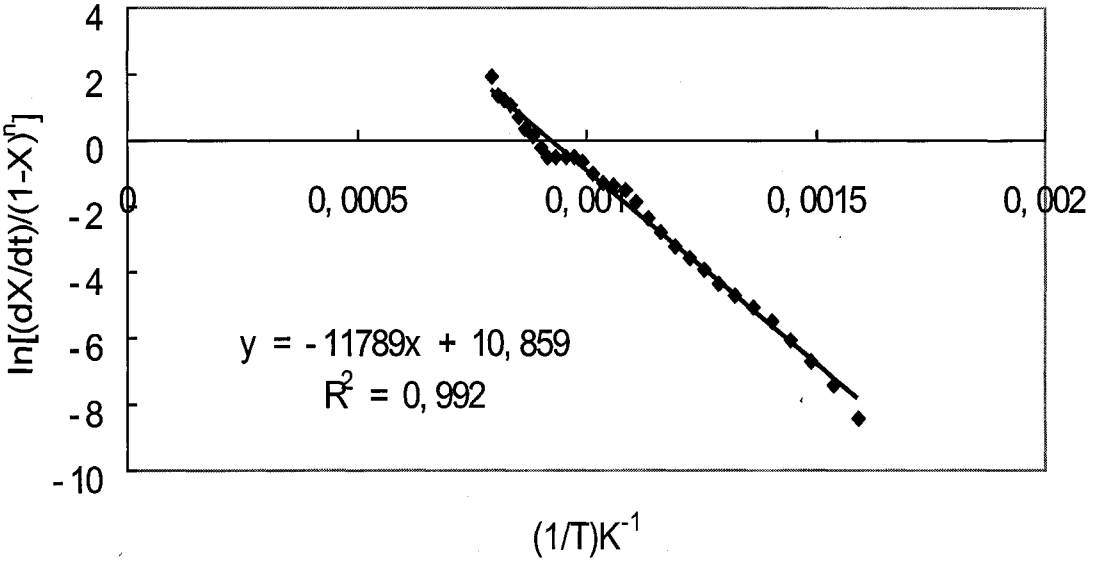

Figure 6.17 Determination of kinetic parameters of methane for anode 1

Table 6.2 The cumulative results of five baking tests

Anode	1	2	3	4	5
Total (g/100 sample)	6.53	6.28	6.73	6.96	7.69
Hydrogen (g/100 sample)	1.64	1.49	1.52	1.89	2.51
Methane (g/100 sample)	0.53	0.82	0.62	0.56	0.70
Tar (g/100 sample)	4.36	3.98	4.58	4.51	4.48

Table 6.3 Summary of kinetic analysis results

Anode	**Hydrogen**	**Methane**	**Condensable Gas**
1	n=2.6 E=102545 k_0,app =20452 R^2=0.97	n=1.9 E=98014 k_0,app =15200 R^2=0.99	n=1.5 E=40930 k_0,app =1.1 R^2=0.96
2	n=2.1 E=95254 k_0,app =12900 R^2=0.98	n=1.8 E=91454 k_0,app =8860 R^2=0.94	n=1.3 E=38244 k_0,app =0.84 R^2=0.95
3	n=2.5 E=94854 k_0,app =10900 R^2=0.98	n=2.4 E=93084 k_0,app =9650 R^2=0.98	n=1.5 E=37563 k_0,app =0.67 R^2=0.96
4	n=2.9 E=92452	n=2.6 E=95195	n=1.7 E=41666

	k_0,app =7930 R^2=0.97	k_0,app =13000 R^2=0.98	k_0,app =1.6 R^2=0.97
Average values for anodes 1 to 4	**n=2.5** **E=96276** **k_0,app=13046**	**n=2.2** **E=94437** **k_0,app=24726**	**n=1.5** **E=39600** **k_0,app=1.1**
5 **(Lower heating rate)**	**n=2.7** **E=95021** **k_0,app =6570** **R^2=0.93**	**n=2.6** **E=66500** **k_0,app =444** **R^2=0.96**	**n=1.7** **E=47906** **k_0,app =4.36** **R^2=0.95**

6.3 Discussion of results

Thermogravimetric experiments showed that, at constant maximum baking temperature, increasing the baking time (i.e. the heating rate is decreased) improved the baked anode properties under the conditions used during this study. The air permeability value decreased and CO_2 and air reactivity values decreased (percent residuals increased). Thus, from the results of the anode baking, it was found that the two most important baking parameters are baking time (heating rate) and maximum baking temperature. The anode properties seem to improve with increasing total baking time (decreasing heating rate) and maximum baking temperature. However, there are also two factors that need to be taken into account. They are the anode overbaking and the prodution cost. Therefore, anode 4 (see Table 6.1) baked using the highest maximum temperature and regular baking time had the best properites. In addition, the high temperature is also good for volatile combustion. It can be said that within thermogravimetric experiments, a balance of baking and cost was

found not only to improve the properties but also to avoid overbaking and to keep the baking time in an acceptable range.

On the other hand, the knowledge on the release of pitch volatiles forms the basis of energy efficiency improvement in the anode baking process. If the volatiles can be burnt as much as possible within the heating section in the baking furnace, the cost of the energy can be reduced by reducing the fuel. This information also can be used as an input in the baking furnace models. Since their behaviour depends on the raw materials used, they have to be measured specifically for a given anode.

For the experiments for which similar baking conditions were used, the kinetic parameters of the non-isothermal regions are similar. The slight differences are due to different maximum temperatures and soaking times used as well as the non homogeneous nature of anode samples. However, when a lower heating rate was used (anode 5) for the baking, H_2 forms at a faster rate at lower temperatures compared to the other anodes. Two constant-rate H_2 formation zones were observed. When low heating rate was used, CH_4 evolves also at lower temperatures. Then, its concentration suddenly drops and decreases faster compared to the other anodes. Tar seems least affected by the change in heating rate. However, the total amount of tar released (the area under the curve) is smaller if a lower heating rate is used. One reason might be that, at lower heating rate, there is more time for condensable gas to crack.

Kinetic data obtained is useful for predicting the amount, time, and temperature of volatiles. This information can be used to wisely control the combustion of volatiles in the baking furnace and save energy.

6.4 Summary

In this chapter, the baking conditions resulting in improved anode properties were determined. Increasing maximum baking temperature and decreasing baking time (i.e. lowering heating rate) improves the properties. However, optimization is necessary in order to avoid high baking costs and overbaking.

The hydrogen, methane, and tar could be utilized as a source of energy during baking by burning them in air within the flue. Thus, the proper combustion of volatiles can reduce the baking cost. However, this requires some feedback mechanisms and may lead to some modifications in the baking furnace design/firing technique.

Chapter 7

Conclusions and Recommendations

7.1 Conclusions

In this thesis, a small particle recipe (#11) was developed. This composition gave better results compared to those of the base recipe. The anodes with the new composition had less tendency to react with CO_2 and air. Keeping the total baking time constant, when the maximum baking temperature was increased, it was observed that there was improvement in baked anode properties for the samples studied. The air permeability and the CO_2 and air reactivity values decreased (percent residues increased). Thus, the anodes with a higher maximum baking temperature (for the same total baking time) had less tendency to react with CO_2 and air under our test conditions. With TGA, it was observed that the rate of formation of tar was less for lower heating rate.

With TGA, it was observed that the rate of formation of CH_4 was high at lower heating rate. It was also observed that most of the CH_4 was formed at an early temperature range when compared with the results of those at higher heating rate.

Again with TGA, it was observed that the rate of devolatilization of H_2 was less at lower heating rate. But the total amount of hydrogen per 100 gm of sample was found to be more for lower heating rate compared to the results of anodes baked under other conditions.

The average percentage of total weight loss of those 4 tests with the heating rate of 17.5°C/h was 6.74%. Within the total weight loss, the percentage of hydrogen was around 25% in the total volatile components, the percentage of methane was around 8% in the total volatile components and the percentage of tar was around 67% in the total volatile components.

The percentage of total weight loss of anode 5 with the heating rate of 10°C/h was 7.69%. Within the total weight loss, the percentage of hydrogen was 33% in the total volatile components, the percentage of methane was around 9% in the total volatile components, and the percentage of tar was around 58% in the total volatile components. Thus the significant advantage of using lower heating rate was availability of more H_2 and less tar.

For the same maximum baking temperature, when the total baking time was increased (i.e. the heating rate is decreased), it was observed that there was improvement in baked anode properties for the samples studied. The air permeability decreased, and CO_2 reactivity and air reactivity residues increased. However, the increase in total baking time means increased cost. For the same total baking time, when the maximum baking temperature was increased, it was found that there was improvement in baked anode properties for the samples studied. The air permeability value decreased, and % CO_2 reactivity and air reactivity residues increased. Although baking parameters affect the reactivity and permeability of anodes, it seems that they influence the CO_2 reactivity more than the air reactivity. Permeability was affected most by the baking temperature. It can be

said that the best conditions for the baking were thus found to be the highest possible maximum baking temperature and increased baking time

The hydrogen, methane, and tar could be utilized as a source of energy during baking by burning them in air within the flue. Thus proper utilization of the volatiles can reduce the baking cost. The proper utilization of the volatile combustion requires some feedback mechanisms and some changes in the baking furnace design and firing technique.

7.2 Recommendations

Further studies could be undertaken on the recipe formulation in order to further improve the anode properties by varying dry aggregate composition as well as pitch.

The percentage of tar is high in the anode baking volatile components. It would be interesting to study the correlation between the baking conditions and the efficiency of tar burn in order to improve further the energy saving and more environment-friendly production in the baking process.

Measurements in the baking furnace could help quantify the benefits of better volatile combustion by determining the efficiencies under different burning profiles.

REFERENCES

1. Kirstine L. Hulse, Raymond C. Perruchoud, "Process adaptations for finer dust formulations: mixing and forming". Light Metals pp. 467-472, 2000
2. W.Schmidt-Hatting, Optimization of the anode carbon consumption with respect to butt recycling, TMS pp. 579-585, 1993
3. "The internal report of Chalco Guizhou branch version 5, 2007"
4. "The internal report of Chalco Guizhou branch version 2, 2009"
5. "The internal report of Chalco Guizhou branch version 2, 2010"
6. Ren Chengqiang, Litie Hu. "Pyrolysis model of pitch", Chemical engineering(China) Vol.35 No.7 pp.27-30, 2007
7. Carine Dubuisson, "Cinetique de la calcination du coke de petrole en atmosphere oxydante" a thesis of Master in University of Quebec at Chioutimi pp.10-12
8. Nathalie Bouchard, "Pyrolyse de divers brais utilisés dansla technologie Sôderberg et analyse des matières volatiles"A thesis of Master in University of Quebec at Chioutimi pp.5-8
9. Kirstine L. Hulse, "Anode Manufacture: Raw Materials Formulation and Processing Parameters", R&D Ltd. Switzerland, 2000
10. Master Thesis of Yongjin Zhao, "The study of optimizing the quality of pre-baked", Central South University , China, 2004

11. Kirstine L. Hulse, Raymond C. Perruchoud, "Process adaptations for finer dust formulations: mixing and forming". Light Metals pp. 467-472, 2000

12. W.Schmidt-Hatting, Optimization of the anode carbon consumption with respect to butt recycling, TMS pp. 579-585, 1993

13. Werner K.Fischer and Raymond C. Perruchoud, "Influence of coke calcining parameters on petroleum coke quality". Light metal, pp. 811-824, 1985

14. Y S Kocaefe, E Dernedde, D Kocaefe, R. Ouellet, Q. Jiao, W. F. Crowell, "A 3D mathematical model fof the horizontal anode baking furnace". Light Metals, pp. 485-489, 1996

15. Raymond C. Perruchoud, "Effect of coke properties and its blending recipe on performances of carbon anode for aluminium electrolysis", Journal of Central South University of Technology Eng. 13 (6), pp. 647-652, 2002

16. D. Kocaefe, A. Charette and L. Castonguay, "Green coke pyrolysis: investigation of simultaneous changes in gas and solid phases", Butterworth Heinemann, Fuel Vol 74 No.6. pp. 791-799. 1995

17. Belitskus, David, Danka, Daniel J. "Effects of petroleum coke properties on carbon anode quality", Journal of Metals Volume 40, Issue 11, pp. 28-29, 1988

18. Akhmetov, N.M., Galeeva, Z.G., Denisenko, Yu.I. "influence of cooling method on quality of heat-treated petroleum cokes" Chem Technol Fuels Oils,Volume 14, Issue 11-12, pp. 869-872, 1978

19. Jiménez Mateos, J.M. , Romero, E. , De Salazar, C.G. "XRD study of petroleum cokes by line profile analysis: Relations among heat treatment, structure, and sulphur content" Carbon Volume 31, Issue 7, pp.1159-1178, 1993

20. Tosta M, R.J., Inzunza, E.M. "Structural evaluation of coke of petroleum and coal tar pitch for the elaboration of anodes in the industry of the aluminum" TMS Light Metals, pp.887-892, 2008

21. Rørvik, S. , Ratvik, A.P. , Foosnæs, T. "Characterization of green anode materials by image analysis" TMS Light Metals pp.553-558 , 2006

22. Wombles, R.H., Baron, J.T. "Laboratory anode comparison of Chinese modified pitch and vacuum distilled pitch" 135th TMS Annual Meeting; San Antonio, TX; Volume 2006, pp.535-540, 2006

23. Dos Santos Batista, J. , Da Silveira, B.I. "Influence of the sodium content on the reactivity of carbon anodes" Materials Research Volume 11, Issue 3, pp.387-390, 2008

24. Hume S.M. "Anode Reactivity - Influence of Raw Material Properties". 2 ed. Sierre, Switzerland: R&D Carbon Ltd.; 1999.

25. Hume, Sheralyn M., Fischer, Werner K., Perruchoud, Raymond C., Metson, James B., Baker, R.Terry K. "Influence of petroleum coke sulphur content on the sodium sensitivity of carbon anodes" Light Metals: Proceedings of Sessions, TMS Annual Meeting, Warrendale, Pennsylvania, pp. 535-541, 1993

26. Fischer, Werner, Perruchoud, Raymond. "Interdependence between properties of anode

butts and quality of prebaked anodes" the 120th TMS Annual Meeting; New Orleans, LA, USA; February 17-21 , Light Metals, pp.721-724, 1991

27. Schmidt-Hatting, W., Kooijman, A.A., Perruchoud, R. "Investigation of the quality of recycled anode butts" the 120th TMS Annual Meeting; New Orleans, LA, USA; February 17-21 , Light Metals, pp.705-720, 1991

28. Perreault, Nathalie, Cote, Jean-Pierre, Grondin, Eric. "Dust control technology for anode butt recycling" 1997 TMS Annual Meeting; Orlando, FL, USA; February 10-13 , Light Metal, pp. 615-618, 1997

29. Turner, N.R. "Relative contributions from the binder and the aggregate to oxidation impurity levels in a model anode binder matrix" TMS Annual Meeting; New Orleans, LA,USA; pp. 701-707,2000

30. Dagoberto S.S. "Recent developments in anode baking furnace design", Light Metals pp.853-858, 2011

31. Detlef Maiwald. "The development of anode baking technology from past to future", Light Metals, pp. 947-952, 2007

32. R.T Bui, A.Chartte. "Simulating the process of anode baking used in Aluminium Industry", Metallurgical Transactions B, volume 15, issue 3, pp 487-492, 1984

33. Dengcheng Bai, Weirong Zhao. "The internal report of Chalco Guizhou branch version 5", pp. 806-808, 2007

34. D.Maiwald, D.Di Lisa "conversion of the firing and control system and the impact on

the efficiency of the baking process" Aluminium world 2008

35. Felix Keller and Peter O. Sulger, Anode baking, Sierre, Swizerland, R&D Carbon Ltd.2008

36. Stein Rorvik, Lorentz Petter Lossius, "Determination of coke calcinations level and anode baking level application and reproducibility of L-SUB-C based methods" Light metals, pp.841-846, 2011

37. Les Charles Edwards, Keith J Neyrey, and lorentz Petter Lossius, "A review of coke and anode desulfurization", Light Metals, pp.958-962, 2007

38. Dernedde, E., Charette, A. "Kinetic phenomena of the volatiles in ring furnaces", Light Metals, pp. 638-642, 1986

39. http://en.wikipedia.org/wiki/Polycyclic_aromatic_hydrocarbon.

40. David Beach. "Proven control philosophy and operation for anode baking process", Light Metals, pp. 953-957, 2007

41. Maiwald, D. "Full control of pitch burn during baking: It's impact on anode quality, operational safety, maintenance and operational costs", Light Metals, pp. 875-880, 2011

42. http://rd-carbon.com/laboratory_test_equipment___calibration_standards.3.html

43. Beatriz Vry, Ciro kato,"Past quality improvements at ALCOA Pocos de Caldas plant", Light Metal, pp.907-912, 2011

44. M.McClung, J.A.Ross and G.Chovanec, "A method to determine the optimal baking level of carbon anodes", Light Metal, pp.473-480, 2011

45. Colin P Hughes, "Methodes for determining the degree of baking in anodes", Light Metal, pp.521-527, 1996

46. Marianne Aanvik, Morten Sorlie, "Reactivity and texture of cokes doped with aluminum compounds", Light Metal, pp.555-561, 2011

47. Hume S.M. "Anode Reactivity - Influence of Raw Material Properties". 2 ed. Sierre, Switzerland: R&D Carbon Ltd.; 1999.

48. Roy A.Cahill, Ralph E. Gehlbach, "Factors influencing the carboxy reactivity of calcined coke" ,Light Metal, pp.563-568, 2000

49. G.J. Houston and H.A.Oye, "Reactivity testing of anode carbon materials" Light Metal pp.885-899, 2001

50. Tosta M, R.J., Inzunza, E.M. "Structural evaluation of coke of petroleum and coal tar pitch for the elaboration of anodes in the industry of the aluminum" TMS Light Metals, pp. 887-892, 2008

51. Tabereaux, A.T., Richards, N.E., Satchel, C.E. "Composition of reduction cell anode gas during normal conditions and anode effects", TMS Light Metal, pp. 325-333, 1995

52. Rechsteiner Jr.,C., Carlson, M. , Crandall, J., "Rethinking, then re-engineering gas chromatography" Proceedings of the Annual ISA Analysis Division Symposium, pp. 1-13, 2001

53. Teng, S.T.,Williams, A.D.,Urdal, K. "Detailed hydrocarbon analysis of gasoline by GC-MS (SI-PIONA)" J. High Res. Chromatogr.,17(6),pp. 469-475, 1994

54. W.K.Fischer, The interdependence of pitch content, dust fineness,mixing; temperature and kind of raw materials in anode formulation,TMS Paper Selection LM-80-73, 1997

55. Foosnaes Trygve and Naterstad Tormod, "Apparatus and method for direct measurement of coal ash sintering and fusion properties at elevated temperatures and pressures", Light Metal, pp. 407-411,1993

56. Adams, A. N.Mathews, J. P.Schobert, H. H. "The use of image analysis for the optimization of pre-baked anode formulation" Light Metal TMS pp. 547-552, 2002

57. Tabereaux, A.T., Richards, N.E., Satchel, C.E. "Composition of reduction cell anode gas during normal conditions and anode effects", TMS Light Metal, pp. 325-333, 1995

58. Rechsteiner Jr.,C., Carlson, M. , Crandall, J., "Rethinking, then re-engineering gas chromatography" Proceedings of the Annual ISA Analysis Division Symposium, pp.1-13, 2011

59. Teng, S.T., Williams, A.D., Urdal, K. "Detailed hydrocarbon analysis of gasoline by GC-MS (SI-PIONA)", J. High Res. Chromatogr.,17(6), pp. 469-475, 1994

Appendix A

Condensation of tar in TGA-GC system

A successful condensation of the condensable pitch volatiles is one of the key points during baking process using by TGA-GC system. The condensable part of pitch volatiles may stick to the tubes, pipes, and rotameters of TGA and GC. This might block the connections between TGA and GC and cause the suction of the pump to drop and stop the flow of the sampling gas. Thus, the condensation system needs to be operated properly. Figure A.1 and Figure A.2 show the design of the condensation system and the cooling system.

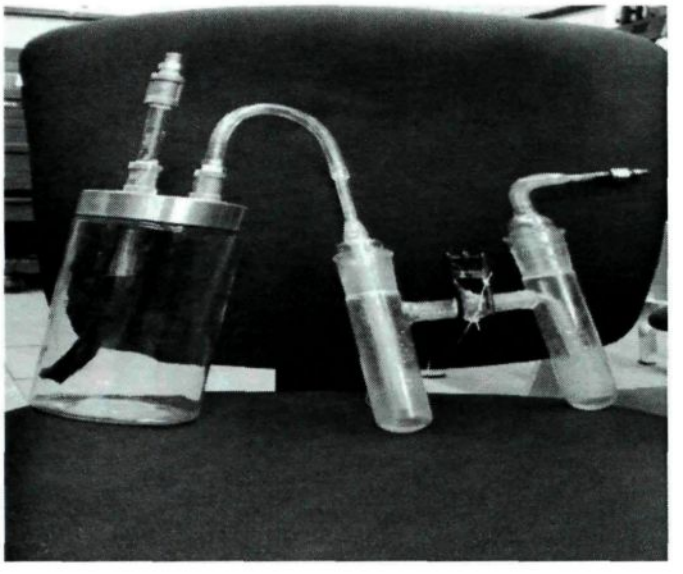

Figure A.1 Condensation system

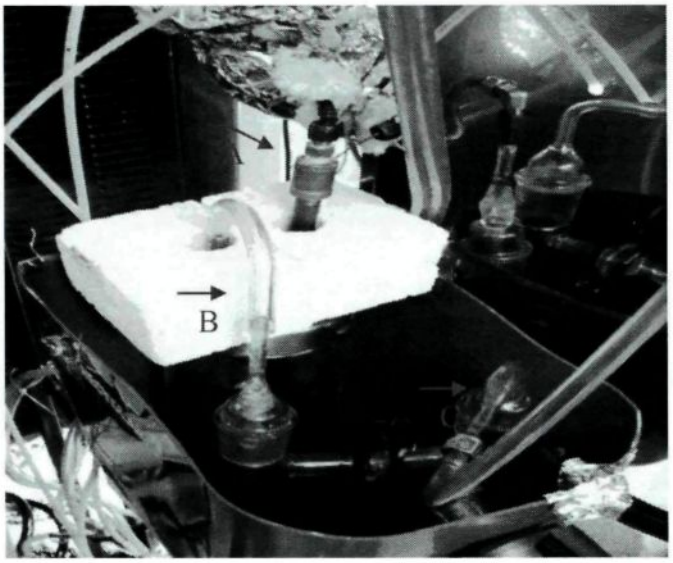

Figure A.2 Cooling system

Figure A.1 shows the condensation system, a big bottle connected to two coupled condensers. Figure A.2 shows the condensation system set-up in the cooling system. Cooling is achieved by the recycling cold water with a temperature of less than 4°C in the blue container. The hot gases are kept at high temperature till they enter the bottle A to avoid any condensation. The condensation takes place in coupled bottles A and B. Then, the non-condensable gases (H_2 and CH_4) pass through C almost without any condensation. The bottles need to be cleaned up during experiment.

Appendix B

The Gas Chromotograph (Varian CP 3380)

The coupling between the TGA and GC was already discussed in Chapter 3. Figure B.1 shows further details of the gas chromotograph operation and various gas flow configurations. The carrier gas was nitrogen. The valve was operated using compressed air. The figure shows the fill state and the inject state of the valve. At the fill state of valve, the carrier gas with the sample gas flows directly into the column. In this case, the injector type 1061 was used for testing gases. The column was 13X molecular sieve. This type of column can separate hydrogen and methane. Column first adsorbes all gases and then desorbes each component separately. The concentration is determined by comparing the thermal conductivity of the sample gas containing carrier gas with that of the reference gas (carrier gas nitrogen) in the detector. The Wheatstone bridge arrangement is used for the thermal conductivity detector measurements.

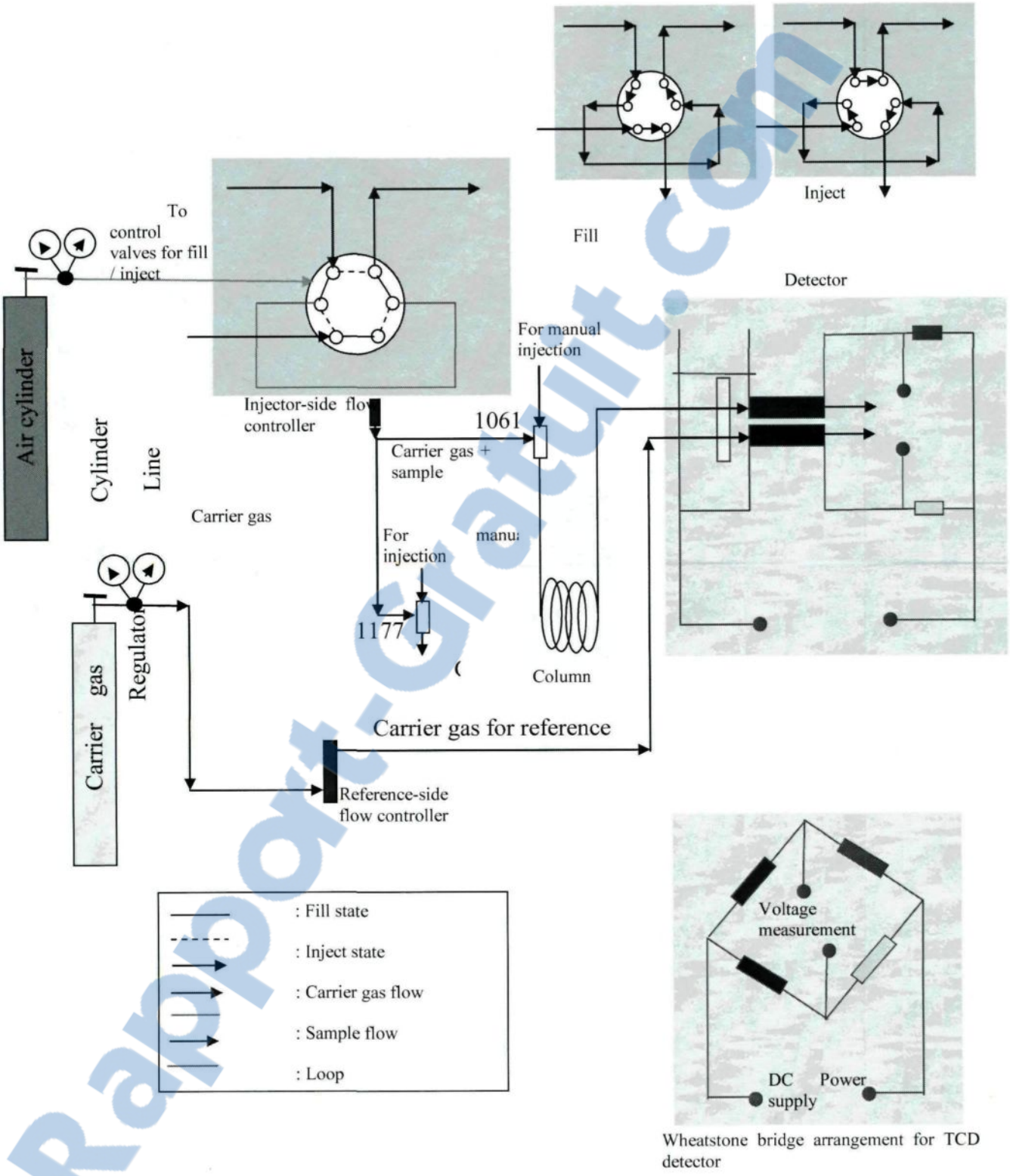

Wheatstone bridge arrangement for TCD detector

Figure B.1 A schematic diagram of the gas chromotograph (GC)

Appendix C

Thermogravimetric Analyser

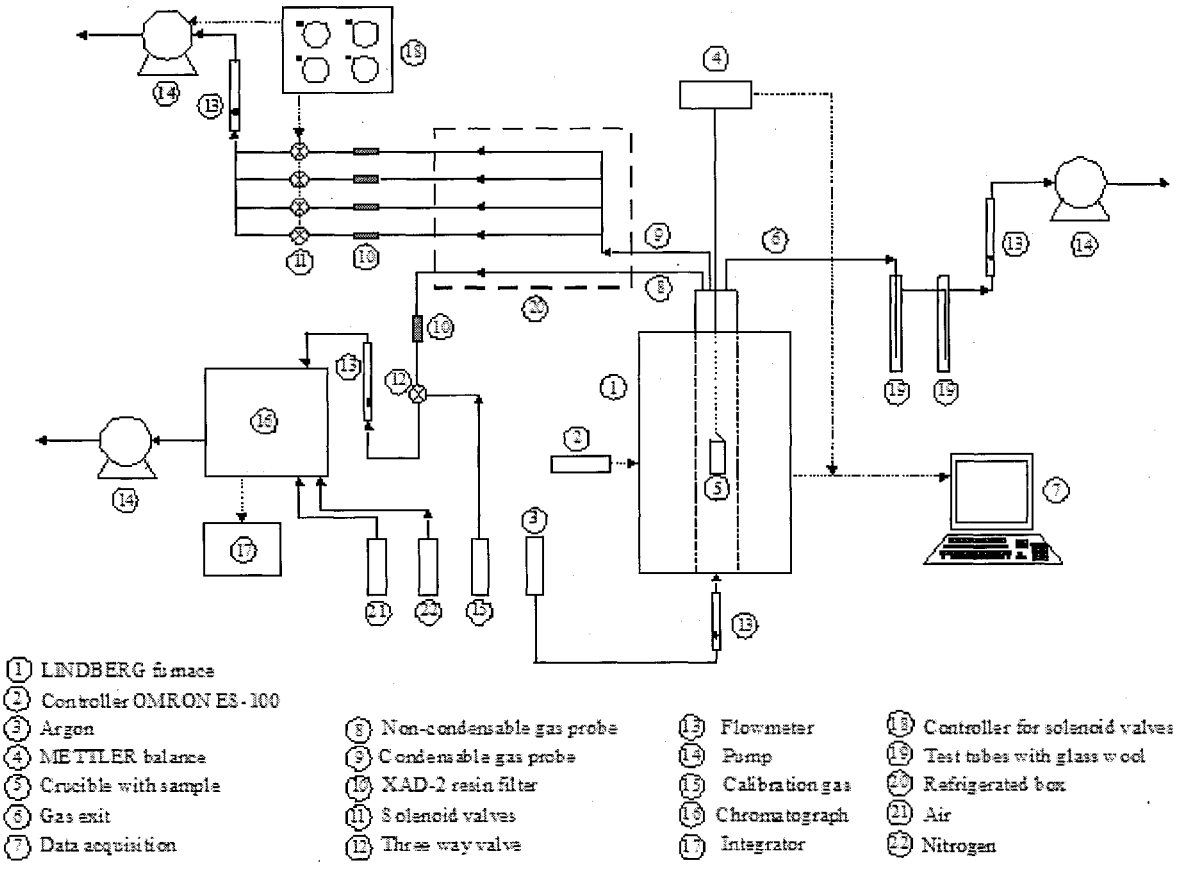

Figure C.1 A schematic diagram of the thermogravimetric analyser coupled with the gas chromotograph

Figure C.1 shows a schematic diagram of the overall system of the thermogravimetric analyser coupled with the gas chromotograph. A more detailed figure was also presented in Chapter 3 (Figure 3.12). A part of the outlet gas is withdrawn for analysis. This gas first

passes through an ice bath to collect the condensable gas. Then, its methane and hydrogen content is analysed using a gas chromatograph (Varian CP 3380) equipped with a thermal conductivity detector. The detector response is calibrated for methane, hydrogen, and oxygen using calibration gases of known concentrations. Data on oxygen was used to detect if there is any air leak on the line and to correct the gas concentration if necessary.